UNIVERSITY OF TURKU

GINGIVAL TISSUE ATTACHMENT AND BLOOD RESPONSES TO NANOPOROUS BIOACTIVE COATINGS ON ZIRCONIA

Khalil Shahramian

TURUN YLIOPISTON JULKAISUJA – ANNALES UNIVERSITATIS TURKUENSIS
SARJA - SER. D OSA - TOM. 1416 | MEDICA - ODONTOLOGICA | TURKU 2019

Gingival Tissue Attachment And Blood Responses To Nanoporous Bioactive Coatings On Zirconia

by

Khalil Shahramian

TURUN YLIOPISTO
UNIVERSITY OF TURKU
Turku 2019

From the University of Turku, Faculty of Medicine, Institute of Dentistry, Department of Prosthetic Dentistry and Stomatognathic Physiology, Finnish Doctoral Program in Oral Sciences (FINDOS-Turku) Turku, Finland.

University of Turku
Faculty of Medicine
Institute of Dentistry, Department of Prosthetic Dentistry and Stomatognathic Physiology
Finnish Doctoral Program in Oral Sciences (FINDOS-Turku)
Turku, Finland

Supervised by

Professor Timo Närhi
Department of Prosthetic Dentistry and Stomatognathic Physiology
Institute of Dentistry, University of Turku
Turku, Finland

Dr. Aous Abdulmajeed
Department of General Practice, School of Dentistry
Virginia Commonwealth University
Richmond, Virginia

Reviewed by

Professor Timo Sorsa
Department of Periodontology
University of Helsinki
Helsinki, Finland

Professor Håvard J Haugen
Department of Biomaterials
Institute for Clinical Dentistry, University of Oslo
Oslo, Norway

Dissertation opponent

Professor Klaus Gotfredsen
Department of Odontology
School of Dentistry, University of Copenhagen
Copenhagen, Denmark

The originality of this thesis has been verified in accordance with the University of Turku quality assurance system using the Turnitin Originality Check service.

ISBN 978-951-29-7596-9 (PRINT)
ISBN 978-951-29-7597-6 (PDF)
ISSN 0355-9483 (Print)
ISSN 2343-3213 (Online)
Grano Oy - Turku, Finland 2019

“In the name of God, the Most Gracious, the Most Merciful”

To my beloved family and mentors

ABSTRACT

Khalil Shahramian

Gingival tissue attachment and blood responses to nanoporous bioactive coatings on zirconia

University of Turku, Faculty of Medicine, Institute of Dentistry, Department of Prosthetic Dentistry and Stomatognathic Physiology, Finnish Doctoral Program in Oral Sciences (FINDOS-Turku), Turku, Finland 2018.

Zirconia implant abutments have gained popularity over the past few years as a substitute for the traditionally used titanium alloy abutments. However, research on the soft-tissue responses of zirconia and improving the zirconia surface properties towards immediate soft-tissue integration are limited.

This series of *in vitro* studies aimed at evaluating tissue and cellular responses of commercially available zirconia versus zirconia provided with sol-gel derived TiO_2 coating. Final purpose of the research project was to optimize zirconia surface properties for fabrication of implant abutments, which enhances gingival tissue attachment.

Coatings were prepared from tetraisopropyl orthotitanate solution by dip-coating method. The effect of coatings and the coating process on the mechanical properties of zirconia was evaluated by biaxial-flexural strength test. Human gingival epithelial and fibroblast cell responses – adhesion kinetics, adhesion strength, and proliferation– was studied in cell culture environment. Blood response, including blood clotting ability, protein adsorption and platelet adhesion and morphology was evaluated. A novel tissue culture method, developed earlier by the research group, was used to evaluate porcine gingival tissue attachment on the coated and non-coated zirconia implants. Adhesion was evaluated using routine microscopy coupled with immunohistochemical staining. Furthermore, the strength of bond between tissue and implants was analyzed utilizing dynamic mechanical analysis.

The biaxial flexural strength of zirconia specimens was unaffected by the coating process. Significant differences were observed in blood coagulation between the coated and non-coated zirconia surfaces. UV treatment of the TiO_2 coated specimens enhanced blood coagulation. Blood platelets also appeared at a higher activation state on coated specimens although no differences in protein adsorption were observed. TiO_2 coated zirconia were significantly more hydrophilic with higher total surface free energy than non-coated ones. Cell proliferation and adhesion was significantly higher on coated specimens. Microscopic observation of gingival tissue attachment on coated implants identified laminin-γ-2 at the attachment of epithelium to implant indicating direct attachment. This observation was absent in non-coated zirconia controls. Furthermore, gingival tissue attachment to coated zirconia implants demonstrated higher dynamic modulus of elasticity and higher creep modulus.

Sol-gel derived TiO_2 coatings on zirconia enhance trombogenicity and facilitate direct gingival tissue attachment on zirconia surface. These findings indicate that TiO_2 coating on zirconia abutments has good potential to improve implant treatment results.

Keywords: Blood, Dental materials, Epithelial cell, Fibroblast, Gingival tissue, Immunohistochemistry, Implant abutment, Mechanical strength, Sol-gel, Surface free energy, Tissue culture, Zirconia.

TIIVISTELMÄ

Khalil Shahramian

Ienkudoksen kiinnittyminen ja veren reaktiot zirkonian nanoporottisessa bioaktiivisessa pinnoitteessa

Turun yliopisto, lääketieteellinen tiedekunta, hammaslääketieteen laitos, hammasprotetiikka ja purentafysiologia, Finnish Doctoral Program in Oral Sciences (FINDOS-Turku), Turku, Suomi 2018.

Zirkoniasta valmistettujen implantti abutmenttien suosio on viimevuosina kasvanut perinteisesti käytettyjen titaaniyhdisteistä valmistettujen abutmenttien vaihtoehtona. Tutkimustyö zirkonian kudosreaktioista ja zirkonian pintaominaisuuksien parantamisesta välittömän pehmytkudosliitoksen aikaansaamiseksi on ollut vähäistä.

Näiden *in vitro* olosuhteissa tehtyjen tutkimusten tavoitteena oli selvittää kaupallisen ja sooli-geeli menetelmällä TiO_2 pinnoitettujen zirkonia materiaalien kudos- ja solureaktioita. Tutkimusprojektin tavoitteena oli optimoida zirkonian pintaominaisuuksia ienkudoksen kiinnittymistä parantavien abutmenttien valmistusta varten.

Pinnoitteet valmistettiin tetraisopropyyli orototitanaatti liuoksesta dippausmenetelmää käyttäen. Pinnoitteen ja pinnoitusprosessin vaikutus zirkonian mekaanisiin ominaisuuksiin selvitettiin biaksiaalisella taivutuslujuustestillä. Ihmisen ienkudoksen epiteeli- ja fibroblastisoluilla selvitettiin solujen vastetta - tarttumista, kiinnittymistä ja kasvua - soluviljelyolosuhteissa. Veren reaktioiden osalta tutkittiin hyytyminen, proteiinien adsorptio sekä verihiutaleiden tarttuminen ja niiden morfologia. Tutkimusryhmän aiemmin kehittämää uutta kudosteknologista mallia käytettiin analysoimaan sian ienkudoksen kiinnittyminen pinnoitettuun ja pinnoittamattomaan zirkonia implanttiin. Kiinnittymistä arvioitiin perinteistä mikroskopiaa sekä immunohistokemiallista värjäystä käyttämällä. Ienkudoksen kiinnittymisen mekaaninen lujuus implanttien pinnoille selvitettiin dynaamisen mekaanisen testin avulla.

Pinnoitusprosessi ei vaikuttanut zirkoniasta valmistettujen testikappaleiden biaksiaaliseen taivutuslujuuteen. Veren hyytymisnopeudessa todettiin merkittäviä eroja pinnoitettujen ja pinnoittaminen zirkonia pintojen välillä. TiO_2 pinnoite lisäsi merkittävästi veren hyytymisnopeutta. TiO_2 pinnoitteiden UV käsittely nopeutti edelleen veren hyytymistä. Näytteiden pinnalle kiinnittyneet verihiutaleet olivat aktiivisemmassa vaiheessa pinnoitetuilla näytteillä pinnoittamattomiin verrattuna, mutta proteiinien kiinnittymisessä ei havaittu eroja. TiO_2 pinnoitetut näytteet olivat merkittävästi hydrofiilisempia ja niiden vapaa pintaenergia oli selvästi suurempi pinnoittamattomiin näytteisiin verrattuna. Solujen jakautuminen ja tarttuminen oli parempi pinnoitetuilla näytteillä. Mikroskooppisessa tutkimuksessa ienkudoksessa todettiin laminiini-γ-2 ilmeneminen epiteelin ja implantin rajapinnalla, mikä viittaa välittömän kudosliitoksen muodostumiseen. Tätä ei havaittu pinnoittamattomilla zirkonia kontrolleilla. Ienkudoksen kiinnittyminen pinnoitettuihin zirkonia implantteihin voitiin osoittaa lisäksi suuremman dynaamisen elastisen- ja vetomoduluksen muodostumisen kautta.

Sooli-geeli menetelmällä valmistettu TiO_2 pinnoite parantaa veren trombogeenisyyttä ja mahdollistaa ienkudoksen välittömän tarttumisen zirkonian pinnalle. Nämä havainnot viittaavat siihen, että TiO_2 pinnoitetut zirkonia abutmentit ovat potentiaalisia parantamaan implanttihoidon lopputulosta.

Avainsanat: Veri, hammaslääketieteen materiaali, epiteelisolu, fibroblasti, ienkudos, immunohistokemia, implantti abutmentti, mekaaninen lujuus, sooli-geeli, vapaa pintaenergia, kudosviljely, zirkonia.

LIST OF ABBREVIATIONS

AFM	Atomic force microscopy
ANOVA	Analysis of variance
°C	Degrees Celsius
CAD/CAM	Computer-aided design/Computer-aided manufacturing
FP	Fractional polarity
JE	Junctional epithelium
MPa	Megapascal
N	Newton
n	Number of specimens per group
PEEK	Polyetheretherketone
PIE	Peri-implant epithelium
PSZ	Partially stabilized zirconia
SEM	Scanning electron microscopy
SFE	Surface free energy
SD	Standard deviation
Y-TZP	Yttria-stabilized tetragonal zirconia polycrystals
UV	Ultraviolet light

LIST OF ORIGINAL PUBLICATIONS

I. **Shahramian K**, Leminen H, Meretoja V, Linderbäck P, Kangasniemi I, Lassila L, Abdulmajeed AA, Närhi T. Sol-gel derived bioactive coating on zirconia: effect on flexural strength and cell proliferation. Journal of Biomedical Material Research Part-B. 2017.

II. **Shahramian K**, Abdulmajeed AA, Kangasniemi I, Soderling E, Närhi T. TiO_2 coating and UV photofunctionalization enhances blood coagulation on zirconia surfaces. BioMed Research International. *In Press*

III. Riivari S*, **Shahramian K***, Willberg J, Närhi, T. TiO_2 Modified Zirconia Surface Improves Epithelial Cell Attachment. The International Journal of Oral & Maxillofacial Implants. 2019.

IV. **Shahramian K**, Gasik M, Kangasniemi I, Willberg J, Abdulmajeed AA, Närhi T. Zirconia implant abutments with improved attachment to the soft tissue interface. Dental Materials. *Submitted*

*Equal contribution of first authors.

1. INTRODUCTION

As a result of the research conducted in the past decades, the osseointegration of oral implant materials have become highly predictable and this has made a shift in interest in research testing oral implant materials. The current focus at the time of writing this thesis is at reducing the incidences of peri-implant infections and at achieving better esthetic outcomes. In this context, one important factor is to have an abutment material that attaches to the surrounding gingival tissues. The soft-tissue cuff around an implant abutment functions as a barrier against bacterial invasion and thereby preserves the underlying bone. This is very important for the long-term success of esthetically and functionally pleasant implants.

A lot of research has been conducted to study the gingival attachment to abutment materials and attempts have also been made to develop new, or optimize the available materials, that can truly bond with the surrounding gingival tissue. Since titanium has been traditionally used in implant therapy, majority of such research has focused on optimizing titanium surfaces. One example of optimizing a material is creation of surfaces that favor cell and tissue attachment. For instance, previous in vitro and animal studies have indicated, that sol-gel derived TiO_2 coatings have a potential to improve the soft tissue attachment on titanium (Areva et al., 2004; Meretoja et al., 2010; Rossi et al., 2008; Wennerberg et al., 2011). Sol-gel derived coatings also have additional benefits such as being thinner, non-resorbable and to possess a simpler production procedure compared to other surface treatment techniques (Areva et al., 2004). In addition, they can be readily deposited on geometrically difficult surfaces and have the possibility to incorporate biologically active molecules (Areva et al., 2004).

Among all the alternatives to titanium, zirconia has gained a substantial popularity with the shift in dentistry towards metal-free restorations. The advantageous properties of zirconia as a biomaterial is a consequence of addition of yttria (Y_2O_3) to zirconia (ZrO_2) crystals, that yields what is commonly known as Yttria-stabilized Tetragonal Zirconia Polycrystal (Y-TZP) (Piconi et al., 1998). Once sintered, it has high bending strength and properties that are similar to stainless steel alloys (Piconi et al., 1998; van Brakel et al., 2012). When compared to titanium, zirconia abutments possess better light dynamics and hence, the final prosthesis is more esthetic to the human eye (van Brakel et al., 2012). Moreover, zirconia has been found to elicit less plaque accumulation and also provoke weaker inflammatory responses than titanium (Rimondini et al., 2002; Scarano et al., 2004; van Brakel et al., 2011). Because of this popularity and the increase in use, it is tempting to optimize zirconia abutments for better soft tissue adhesion. However, few or no research has addressed this issue.

The aim of this project is to explore the possibility to apply sol-gel derived TiO_2 coatings on zirconia without weakening its fracture strength. The aim is also to evaluate if TiO_2 coatings can enhance biological processes related to wound healing cascade on zirconia surface.

2. REVIEW OF LITERATURE

2.1. Gingival tissue attachment on tooth and implant surface

The formation of the natural dentition is the result of several complex developmental processes that result in a structural continuity between the different components of the dentition (Ivanovski & Lee, 2018). The tooth per se is composed of enamel and dentin, and the periodontal tissue surrounding the tooth is composed of cementum, periodontal ligaments, gingiva, and the alveolar bone (Listgarten et al., 1991). The main functions of the periodontal tissue is to anchor the tooth in the jaw bone and to provide a seal that separates the contaminated intraoral environment from the aseptic internal environment (Listgarten et al., 1991). The latter is provided by the gingiva, which, in other words, is the soft tissue that surrounds the teeth (Grant, et al., 1987; Listgarten et al., 1991; Schroeder & Listgarten, 1977). A closer microscopic look at this seal shows that it consists of a dento-epithelial junction coronally, and a connective tissue junction apically. The coronal epithelial component can be further divided into two zones, the oral sulcular epithelium and the junctional epithelium. The junctional epithelium consists of two basal laminas, one that attaches to the tooth surface; the internal basal lamina, and one that attaches to the underlying connective tissue; the external basal lamina (Cate & Nanci, 2017). The junctional epithelium is known to have a critical role in tissue homeostasis and defense against the invasion of bacteria or their elements (Bosshardt & Lang, 2005). The apical connective tissue component of the seal is also comprised of two parts, a part that supports the overlying epithelium and a part that interfaces the tooth (the cementum). The part that interfaces the tooth consists of several fibers that are inserted into the tooth cementum in different orientations. These gingival fibers are named and described according to their orientation (Schroeder & Listgarten, 1997). The most dominant type of fiber is the dento-gingival fibers that extend from the cementum to the connective tissue of the free and attached gingiva around a tooth (Cate & Nanci, 2017). Other fibers that attach the gingiva to teeth and bone include the dento-periosteal, alveolo-gingival and periosteo-gingival fiber groups. Moreover, there is interpapillary fibers connecting the vestibular and the interdental papillae, and the circular and transeptal fibers that connect the adjacent teeth to each other (Ivanovski & Lee, 2018). The connective tissue around a tooth is also highly vascularized, a characteristic that is crucial for the inflammatory response and defense mechanisms of the tissue (Schroeder & Listgarten, 1997).

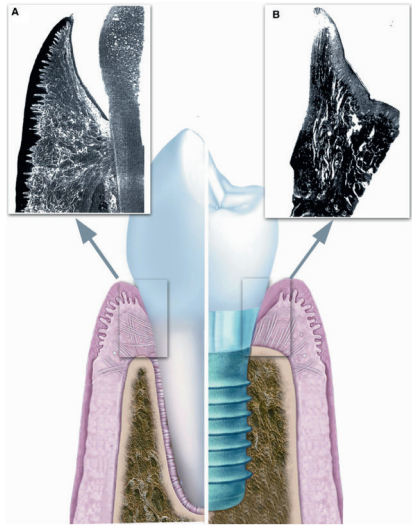

Figure 1*Cross-section of (A) buccal dento-alveolar region; connective tissue fibers inserted into the root. (B) Buccal peri-implant bone and mucosa; no insertion of connective tissue fibers into the implant surface.*
(Source: Ivanovski & Lee (2018))

The tissue that occurs around osseointegrated implants (the bone and the soft tissue) is termed as the peri-implant tissue (Araujo & Lindhe, 2018). It forms during the wound healing process that happens after the surgical placement of implants/abutments (Berglundh et al., 2007). The peri-implant tissue serves two basic functions; the soft tissue protects the underlying bone while the bone supports the placed implant. The structure of the soft-tissue around a dental implant is in many ways comparable with those around the natural dentition (Chai et al., 2010; Ivanovski & Lee, 2018; Listgarten et al., 1991). However, some differences are still evident. It is important to understand that unlike natural teeth that have developed simultaneously with their surrounding periodontal tissues, implants, (inorganic tooth substitute) are artificially placed exogenously in an osseous receptor site (Listgarten et al., 1991; Weber & Cochran, 1998). Implants lack a cementum layer, and this does not allow them to interact in the same way that a tooth does with surrounding tissues. The fibers in the connective tissue around a tooth are predominantly inserted perpendicularly into the cementum, whereas the connective tissue around an implant is comprised of fibers that run primarily parallel to the implant surface (Abrahamsson et al., 1998; Berglundh et al., 1991; Buser et al., 1992; Listgarten et al., 1991; Weber & Cochran, 1998). This means that the connective tissue around an implant has adapted to the surface and is not truly attached. Another difference observed in the connective tissues surrounding implants and teeth is the degree of vascularization. The connective tissue around an implant is very collagenous and is found to be almost lacking a vascular supply when compared to the richly vascularized connective tissue that is in contact with the tooth cementum (Abrahamsson et al., 1998; Buser et al., 1992; Moon et al., 1999; Schupbach & Glauser, 2007; Weber & Cochran, 1998). This inflammation-free scar-tissue structure weakens the defense mechanism of the peri-implant mucosal tissue, making it more vulnerable to harsh bacterial challenges (Ivanovski & Lee, 2018).

2.2. Wound healing around oral implant

Clinically, wound healing around peri-implant and periodontal tissues is not very different. However, in a recent study, Emecen-Huja et al. (2013) demonstrated that on a molecular level some differences are evident. They examined the expression of different inflammatory modulators in peri-implant crevicular fluid and gingival crevicular fluids at early wound healing stage and found that peri-implant tissues generally represent a higher pro-inflammatory state when compared to periodontal tissues. The presence of inflammation is considered to be necessary and important for the wound healing process (Tomasi et al., 2016) and also for the recruitment of inflammatory cells and other chemical mediators that are important in both wound healing and tissue regeneration. On the other hand, a scar tissue forms if the inflammation is prolonged (Sculean et al., 2014). The wound healing around dental implants occurs after the closure of the mucoperiosteal flap that was raised during the surgery (Maté Sánchez de Val et al., 2016). This wound healing process occurs in the presence of a biomaterial that must have behaviors to adapt well to the healing tissue (Sculean et al., 2014).

In summary, the classic wound healing process consists of a hemostatic phase, an inflammatory phase and a tissue regeneration phase (Sculean et al., 2014). Wound healing is kicked-off with the hemostatic phase when the defect site is closed by a blood clot (Dickinson et al., 2013). This blood clot includes blood cells and activated and aggregated platelets, and is sometimes referred to as blood coagulum (Sculean et al., 2014). The cell constituents are entrapped in a matrix composed of fibrin network and other proteins like fibronectin and vitronectin (Clark et al., 2004; Reheman et al., 2005). This whole complex is responsible for attracting inflammatory cells into the site and will be later on replaced by the granulation tissue. The inflammatory phase involves recruitment and activity of neutrophils and monocytes that clear the wound site from invading bacteria and is followed by the phase of new tissue formation, where a highly vascularized tissue made of fibroblasts initiates the process of tissue regeneration (Sculean et al., 2014). The tissue that is formed later on remodels and often ends up as scar tissue due to apoptosis of the majority of fibroblasts and other cells, leaving a collagen-rich matrix devoid of cells.

Wound healing around implants was looked at in a relatively recent animal study by Berglundh et al. (2007). A blood coagulum initially separates the implant placed from the bone or the soft tissues. This coagulum is later infiltrated by cells and replaced by a dense fibrin network that later on gets invaded by fibroblasts that produce collagen fibers and eventually the connective tissue. The newly formed connective tissue is already in close contact with the implant two weeks after the surgery. Epithelial cells' migration to the implant surface occurs one to two weeks after placement and eventually result in the formation of the peri-implant junctional epithelium. The whole barrier matures within 6 to 12 weeks after implant placement, resulting in the anatomy described in section 2.1.

2.3. Peri-implant infections

Peri-implant diseases, including peri-implant mucositis and peri-implantitis, were first described in 1993 at the First European Workshop on Periodontology (Albrektsson & Isidor, 1994). The incidence of peri-implant mucositis is reported to be in about 80% of subjects (50% of sites) restored with implants, and that of peri-implantitis to be in between 28% and 56% of subjects (12–40% of sites) (Lindhe & Meyle, 2008). In another report, Derks and Tomasi (2015) stated that peri-implant mucositis appears in up to

43% of placed implants, whereas the prevalence of peri-implantitis to be around 22%. The following two subheadings will give more insights about these two disease conditions.

2.3.1. Peri-implant mucositis

Peri-implant mucositis is the term that describes an inflammation in the mucosa surrounding an endosseous implant without any loss of the bone supporting the implant. The important criteria for identifying this condition is the presence of inflammation in the absence of peri-implant bone loss (Albrektsson et al., 1994; Lindhe & Meyle, 2008; Zitzmann & Berglundh, 2008). Peri-mucositis is believed to be the prerequisite for peri-implantitis, which is when the inflammatory lesion is coupled with loss of the bone supporting the implant. The clinical signs of peri-implant mucositis include redness, swelling, bleeding on gentle probing and suppuration of the gingiva surrounding the implant (Heitz-Mayfield & Salvi, 2018).

Healthy peri-implant mucosa converts to peri-implant mucositis following the accumulation of a bacterial biofilm around the osseointegrated implant. Experimental peri-implant mucositis in humans has established a cause-and-effect relationship between the accumulation of bacterial biofilms and development of this inflammatory response (Meyer et al., 2017; Pontoriero et al., 1994; Salvi et al., 2012; Zitzmann et al., 2001). This finding is consistent with the cause-and-effect relationship demonstrated with the results of experimental gingivitis studies linking the onset of gingivitis to bacterial biofilm accumulation (Löe et al., 1965; Meyer et al., 2017; Pontoriero et al., 1994; Salvi et al., 2012; Zitzmann et al., 2001). However, in comparison to the mucosa around teeth accumulating bacterial biofilms, peri-implant mucosa is more prone to development of peri-implant mucositis and is found to have a more severe inflammatory response when exposed to a comparable bacterial challenge. The trueness of this cause-effect relationship was demonstrated by Salvi et al. (2012) where the inflammatory state and condition was reversed to the pre-experimental levels when the bacterial biofilm in test subject were controlled by reinstituting oral hygiene practices. Furthermore, longitudinal studies evaluating long-standing peri-implant mucositis lesions have shown that patients who did not adhere to supportive peri-implant therapy had higher incidence of peri-implant mucositis at 5 years (Costa et al., 2012). Among these patients, the prevalence of peri-implant mucositis was reported to be 48% in a period of 9 to 14 years of observation (Roos-Jansaker et al., 2006a, 2006b, 2006c). Treatment of peri-implant mucositis is therefore important to avoid cases of peri-implantitis (Heitz-Mayfield & Salvi, 2018). Furthermore, since the peri-implant mucosa is more prone to a more severe inflammatory response towards the same bacterial challenge than the mucosa around teeth, it is important that implant materials result in a peri-implant mucosa that behaves in the same manner as the mucosa around teeth.

2.3.2. Peri-implantitis

Peri-implantitis, as it was briefly touched upon in the previous section, is the term given to the pathologic condition in the tissue surrounding an implant, with inflammation in the peri-implant mucosa and progressive loss of the bone supporting the implant (Lang & Berglundh, 2011; Lindhe & Meyle, 2008). Clinically, the peri-implant tissue is characterized by signs of inflammation and bleeding on probing and the progressive bone loss is detected by radiographs (Schwarz et al., 2018).

Similar to the progression of gingivitis to periodontitis, the prerequisite for peri-implantitis is peri-implant mucositis (Jepsen et al., 2015). The exact turn over point where peri-implant mucositis converts to peri-implantitis is not yet identified and fully understood. However, there seems to be cause-effect relationship of bacterial colonization and the onset of peri-implant mucositis that may progress in some cases to peri-implantitis. Furthermore, the inflammatory reaction in experimental peri-implantitis in animals is found to be more severe than that in experimental periodontitis (Carcuac et al., 2013). Inflammatory lesions in peri-implantitis are found to be twice as large, have a larger inflammatory cell infiltrate, more severe bone loss, and progress faster than lesions in periodontitis (Carcuac & Berglundh, 2014). The etiology of peri-implantitis is multifactorial and its incidence is different in different individuals. Some risk factors are suggested to be linked to the development of peri-implantitis. There is strong evidence that poor plaque control, inadherence to maintenance care after implant therapy and history of previous chronic periodontitis, serve as a risk factors for developing peri-implantitis (Costa et al., 2012; Roccuzzo et al., 2012). Other factors like presence of excess submucosal cement, lack of peri-implant keratinized mucosa, smoking, and diabetes are still inconclusive in establishing a sound relationship (Renvert & Quirynen, 2015; Schwarz et al., 2018). Furthermore, progressive bone loss around implants is found to be mainly, if not always, accompanied with clinically inflamed supporting soft tissue (Renvert & Quirynen, 2015; Schwarz et al., 2018).

2.4. Abutment materials

Several materials have been used in manufacturing implant abutments. Traditionally titanium has been the material of choice in implant dentistry. However, other materials like alumina, zirconia and polyetheretherketone have been introduced as potential alternatives to titanium. Among these, zirconia has gained an increasing popularity as a substitute to titanium.

2.4.1. Titanium

Commercially pure titanium and titanium alloys have been the gold standard in implant dentistry for the past decades. Titanium has excellent biocompatibility, corrosion resistance and sufficient mechanical properties. However, titanium abutments have been reported to have some drawbacks in certain cases. The increasing demands in esthetics have necessitated the development and use of more esthetically pleasing alternatives to titanium. In addition, titanium can produce artifacts during imaging examinations (Eggers et al., 2005; Kamel et al., 2003). Furthermore, titanium sensitivity in some patients and the gingival discoloration caused by titanium particles are other issues that bring limitations to this material (Andreiotelli et al., 2009; Kajiwara et al., 2015).

2.4.2. Alumina

All ceramic tooth-colored abutments made from densely sintered aluminum oxide were developed for the first time in 1993 (Prestipino & Ingber, 1993a, 1993b). Alumina abutments showed good esthetics and biocompatibility and a healthy mucosa was found around the abutments comparable to the mucosa around titanium abutments (Andersson et al., 2001; Andersson et al., 2003; Henriksson & Jemt, 2003). However, mechanically, alumina abutments have a risk of fracture both during function and laboratory work and this risk have limited their use in implant therapy.

2.4.3. Polyetheretherketone

Polyetheretherketone or in other words PEEK abutments have been proposed as a temporary option to support implant-retained provisional crowns. PEEK is reported to have inert chemical properties and a good biomechanical strength. However, this material is new and more research is required to draw conclusive decisions towards its use in implant therapy (Schwitalla et al., 2015; Schwitalla & Müller, 2013).

2.4.4. Zirconia

Zirconia abutments can be prefabricated or custom milled using CAD/CAM technology in the dental laboratory (Höland et al., 2008; Ritzberger et al., 2010). The use of zirconia abutments is increasing in esthetic regions due to its non-metallic appearance and better matching with the increasingly used all-ceramic crowns. Titanium abutments may show through the peri-implant tissues and give a non-pleasing grayish hue appearance (Yildirim et al., 2000). Short-term clinical trials on zirconia abutments have reported that they could function without fracture in the oral cavity (Guess et al., 2012; Nakamura et al., 2010).

2.4.4.1. Mechanical and optical properties

Zirconia is a polymorphic material existing in three allotropes; monoclinic (m), tetragonal (t) and cubic (c), which are stable at different temperatures. The tetragonal phase exists at high temperatures; however, it can be stabilized at room temperature by the addition of oxides of yttria or ceria to the zirconia structure (Partially stabilized zirconia, PSZ) (Piconi et al., 1998). Different manufacturers have different ratio of chemical compositions that yield in zirconia with variable properties. In general, PSZ has a high flexural strength in the 800-1000 MPa range and fracture toughness in the range of 6-8 MPa $m^{1/5}$ (Denry & Kelly, 2008). This strength lies in the transformations happening in the metastable tetragonal crystalline structure of zirconia at room temperature. When under stress, the tetragonal grains transform into monoclinic with a 3-4% volume expansion. The consequent volume expansion creates compressive stresses that oppose the tensile stresses leading the induced crack, hence preventing further crack propagation (Piconi & Maccauro, 1999; Porter & Heuer, 1977). This phenomenon is termed as "transformation toughening" and gives zirconia its advantageous mechanical properties.

The optical properties of zirconia are affected by its chemical composition, porosity, phase distribution, surface structure, thickness, and light source (Shahmiri et al., 2018). Zirconia has the ability to mask dark substrates. This is because zirconia's grain size is larger than the length of light and it has a high density, a high refractive index, and a low absorption coefficient (Sivaraman et al., 2017). Commercially available partially stabilized zirconia are pure white in color but their color can be adjusted to simulate that of teeth through addition of nano-sized pigments of iron oxide or lanthanum prior to the sintering process (Gahlert et al., 2012; Heffernan et al., 2002; Ivanoff et al., 1997).

2.4.4.2. Zirconia vs titanium

Both titanium and zirconia are bioinert and show good compatibility with their surrounding tissue. Hosseini et al. (2013) compared the clinical outcomes of different abutment materials after 3 years and found no difference between biological outcomes of zirconia and metal abutments. However, peri-implant mucosa surrounding zirconia abutments had less discoloration.

The quality of gingiva surrounding zirconia and titanium abutments is similar. The amount of bleeding on probing and the parallel oblique pattern observed in connective tissue fibers microscopically are often comparable. However, some differences still exist in the tissue. Gingival tissue surrounding zirconia has a longer junctional epithelium and a higher density of collagen fibers. This gives zirconia the advantage of providing a better soft tissue adaptation and thereby reduced bacterial ingression and inflammation when compared to titanium (Nascimento et al., 2014; Scarano et al., 2004). Furthermore, research has shown that zirconia has a lower tendency towards bacterial plaque adhesion and accumulation (Scarano et al., 2004). This property can in turn prevent the development of peri-implant inflammations and eventual bone resorption. In addition to low bacterial colonization, zirconia abutments have reduced inflammatory response in the surrounding tissue compared to titanium (Hisbergues et al., 2008). This indicates that the onset of peri-implantitis can be less frequent with zirconia when compared to titanium (Degidi et al., 2006; Nascimento et al., 2014; Quirynen et al., 1993; Rimondini et al., 2002; Salihoglu et al., 2011; van Brakel et al., 2012).

An important advantage of zirconia over titanium is its excellent esthetic properties and the final prosthesis with zirconia implant abutments is more pleasing to the human eye. A major drawback of zirconia towards titanium can be however, the brittleness of this ceramic material over the latter ductile metal. In this regard, Coray et al. (2016) conducted a systematic review where they evaluated studies reporting the fracture strength of titanium and zirconia abutments after fatigue testing. Fatigue testing involving cyclic loads to materials are more relevant to studying their clinical behavior compared to studies employing static load tests. Although zirconia is expected to behave inferiorly compared to titanium as a result of its weakening because of low thermal degradation phenomenon with time, Coray et al. found no dramatic decrease in the ultimate strength of zirconia in their study sample. However, they further reported that the results need to be evaluated with caution due to the differences and discrepancies in the testing conditions in the literature. In addition, zirconia is relatively new when compared to titanium and long-term clinical trials are necessary to reach an ultimate conclusion with this material. Nevertheless, currently zirconia is being increasingly used in dental practices in different applications, and similar to other materials utilized in manufacturing dental implants, it is important to improve the current state of zirconia/soft-tissue compatibility to support the peri-implant environment and further reduce the incidence and onset of peri-implant diseases.

2.5. Factors influencing gingival tissue attachment on implant surface

Dental implants extend all the way from the oral cavity to the alveolar bone and hence form several interfaces with various tissues (bone, connective tissue, and epithelium) simultaneously. The different parts of the implant system need to have surfaces that are each optimized for their respective function in different environments. For instance, at the soft tissue interface, the surface must have characteristics to favor adhesion and function of keratinocytes and fibroblasts to ensure an epithelial seal that will protect

the osseointegrated implant from bacterial infiltration. It is known that surface characteristics like chemical composition, surface roughness and surface wettability are key parameters for cell adhesion, proliferation and colonization (Abrahamsson et al., 2002; Al-Ahmad et al., 2010; Bürgers et al., 2010; Grossner-Schreiber et al., 2001; Hamdan et al., 2006; Linkevicius & Apse, 2008; Marc Quirynen et al., 1994; Teughels et al., 2006; van Brakel et al., 2011). However, most studies have focused on studying surface properties that improve the implant/bone interface and till this date, our knowledge of the transgingival soft-tissue interface is limited and very elementary.

2.5.1. Chemical composition

Different materials have various surface properties, which makes them behave differently when in contact with body tissues or interstitial fluids. Since the interactions of a material with the tissues or fluids is limited to its surface, surface properties and chemical composition of the material are important parameters to be considered (Rompen et al., 2006). Interestingly, the surface properties might be essentially different from the bulk properties of the material. For example, all commercially available titanium exist with a layer of titanium oxide that forms naturally on the surface at room temperatures, the properties of which are different from titanium metal (Kasemo & Lausmaa, 1985). Furthermore, studies have shown that all available implant abutments have chemical properties that show equal biocompatibility towards the surrounding soft tissue (Degidi et al., 2006; Linkevicius & Apse, 2008; Vigolo et al., 2006). However, zirconia abutments have been reported to give better surface responses to gingival tissues when compared to traditional titanium ones (Nothdurft et al., 2015).

2.5.2. Surface roughness

The surface roughness and topography of dental implants have been under investigation for the past decades and different surface modifications have been introduced to achieve best contact with the surrounding bone (Rupp et al., 2018). An important finding of in vitro and in vivo studies focusing on the bone contact, is that titanium with surface roughness Sa 1-2 μm demonstrates better osseointegration when compared to smooth surfaces (Wennerberg & Albrektsson, 2009). The relation of roughness and anchorage of implants in bone was also shown by Gotfredsen et al. (2000) where rougher implants needed a higher removal torque for removal, translating to a better anchorage in bone. This has also been confirmed in a recent study where osteoblasts were found to have better differentiation and migration on rougher surfaces (Andrukhov et al., 2016). On the other hand, some studies state that fibroblasts prefer smooth surfaces and that a surface roughness of 0.2 μm is considered to be a threshold for soft tissue attachment (Kim et al., 2015). Above this threshold, bacterial biofilms colonize the surface more than cells and tissue. However, there is still little knowledge on how surface roughness parameters are linked with biological responses at implant sites. Currently the methods for surface roughness and topography measurements of implant materials are not standardized and different devices used in evaluation of this surface property make the available data in literature incomparable and conclusion of results difficult (Rupp et al., 2018).

2.5.3. Surface wettability

The surface free energy (SFE) is an indicator of wettability; the higher the SFE, the better the wettability. Research has found that hydrophilic surfaces with high SFE are more favorable for cell responses. Hydrophilic surfaces show significantly higher cell attachment, spreading, and proliferation (Altankov et al., 1996; Ponsonnet et al., 2003; Ruardy et al., 1995; Schakenraad et al., 1988; Webb et al., 1998). Consequently, in the recent years, biomaterials' surface research has started to incorporate studying materials' wetting properties and evaluating its connection with surface topographies when studying tissue response (Rupp et al., 2018).

Surface free energy (SFE) of a solid material is calculated through contact angle measurements made by depositing drops of different liquids on its surface. The contact angles are inserted into the Young equation and the SFE is calculated using different methods resulting the total, polar/apolar or acid/base parts thereof (Rupp et al., 2014; Young, 1805). The polar component of the SFE is known to be of great influence on osteoblasts and other cell behavior. This is because of the polar composition of cells meaning that cells interact with materials mainly in a polar force (Feng et al., 2003; Hallab et al., 1995).

Surface free energy's effect on cell and tissue attachment is also important when considering surface contaminations of abutment or implant surfaces (Rompen et al., 2006). Hydrocarbon contaminations on surfaces are known to reduce the surface energy and interfere with protein adsorption and subsequent colonization by cells (Baier et al., 1984; DePalma et al., 1972; Doundoulakis, 1987; Rupp et al., 2018). Robert E. Baier's group have been pioneers in studying surface cleansing of implants and its influence on surface energy and wound healing properties. Different surface treatments like SLA-active surfaces, plasma treatments or UV irradiation are examples of treatments aimed at removing contaminations that initiate unfavorable attraction of molecules that eventually compromise initial stages of wound healing and result in early marginal bone loss around implants. However, till date, an optimum energetic state for an optimum biological interaction is unsure.

2.6. Methods to improve tissue interactions

Several surface treatments have been studied in order to modify different surfaces on different components of dental implants. These treatments either alter the surface topography or the surface chemistry in order to initiate a faster wound healing process and eventual attachment of tissues (Rupp et al., 2018). It is hypothesized that nanostructured surfaces that can mimic the natural environment of cells may interact with cells on a molecular level and hence influence the processes of cell adhesion, proliferation, differentiation and tissue integration (Rompen et al., 2006; Wennerberg & Albrektsson, 2009). However, most of the studies are directed towards surfaces that will improve the implant/bone interface and studies focused on implant/soft-tissue interface are still limited. Few common surface treatments on titanium are briefly touched upon in this section.

2.6.1. Plasma spraying

Plasma spraying involves spraying high temperature small-sized particles of different substances on to the implant surface (Coelho et al., 2009). This method can be used to deposit coatings of different substances like hydroxyapatite or titanium on to the surface of implants. Research has shown that hydroxyapatite coatings improve initial healing process and show an accelerated bone formation and maturation (Block et al., 1987; Rompen et al., 2006; Thomas et al., 1987). A common drawback observed

with plasma-sprayed coatings is the interface of the substrate surface and the deposited coating. Some reports show delamination or in some cases resorption of the coating (Ong et al., 2004).

2.6.2. Machine-grit blasting

This technique alters the surface topography and roughness of the implant through projection of hard particles like Al_2O_3 or TiO_2 at high velocities onto the surface. This method together with acid-etching is one of the earliest methods that were commercially available as implant surface treatments (Coelho et al., 2009; Lacefield, 1998). The increase in surface roughness of implants is known to improve osseointegration, osteoblast and bone response (Rompen et al., 2006; Rupp et al., 2018).

2.6.3. Acid-etching

The acid etching procedure aims to further enhance the surface topographies and remove contaminants from the surface of the implant (Coelho et al., 2009; Rupp et al., 2018). Acid etching can be performed with or without a previous grit-blasting procedure. Etching agents commonly used are nitric, sulfuric, hydrofluoric, or a combination of different acids (Giavaresi et al., 2003). The acids etch the surface and increase the surface area of the implant. Grit-blasted and acid etched surfaces have been available commercially for a long time. SLA and SLActive surface modified implants by Straumann (Straumann, Basel, Switzerland) are an example of this treatment.

2.6.4. Anodization

Titanium is immersed in a strong acid solution with controlled chemistry and a high current density is passed through it. This alters the surface topography and surface chemistry of titanium by thickening its overlying titanium oxide layer and the subsequent chemical interactions of this layer with the acidic solution (Sul et al., 2002). Several studies have shown the better early response of host tissue to these surface modified implants (Al-Nawas et al., 2007; Sul et al., 2006; Sul et al., 2005; Sul et al., 2002).

2.6.5. Coating

Implants can be coated with various materials or molecules using different techniques. Calcium and phosphorous based coatings have gained much interest in dental and orthopedic implants and a common commercially available coating is hydroxyapatite coating deposited using plasma spraying (Lacefield, 1988, 1998; Lemons et al., 2015; Ong et al., 2004; Park et al., 2005; Yang, Kim, & Ong, 2005). Several other coating methods are also developed for deposition of different coatings on metal implant substrates. Sputter deposition, electrophoretic deposition, physical vapor deposition and chemical vapor deposition are few examples. Hydroxyapatite coatings are also recently deposited using magnetron sputtering method, which falls under the category of physical vapor deposition (Surmenev et al., 2017; Tiwari & Hassan, 2018). Each coating process possess advantages and disadvantages, however, research comparing the clinical performance of different coatings deposited using different methods is still very limited. Another technique is using the dip-coating method using sol-gel. The substrate, in this case the implant, is dipped into a sol-gel solution containing particles of the coating, and then withdrawn, leaving a uniform layer of the coating material on the surface of the implant. The advantage of this procedure to other coating procedures is that the chemical composition of the coating can be more readily controlled.

The precursors are mixed at molecular levels in the solution in which the implant is dipped. The resulting coatings also require lower sintering temperatures in order to be stabilized, when compared to other procedures. Furthermore, the procedure is simple and inexpensive and homogenous coatings can be deposited easily on geometrically challenging surfaces. (Advincula et al., 2006; Areva et al., 2004; Paldan et al., 2008b; Peltola et al., 2000; Wen et al., 2007).

2.6.5.1. Sol-gel derived titanium oxide coatings

Nano-scale TiO_2 particles can be deposited on implant surfaces using the sol-gel dipping method. Previous works of the implant research group at the University of Turku, Jokinen and colleagues and Peltola and colleagues, have shown that these coatings can be potentially beneficial on implant surfaces (Ääritalo et al., 2007; Areva et al., 2007, 2004; Jokinen et al., 1998; Peltola et al., 2000; Rossi et al., 2008). It is known that the nanoscale topography created and the altered chemistry of these coatings, change the reactivity of dental implant surfaces. The coatings are strongly adhered to the underlying implant surface, in contrast to the common drawback observed with plasma-sprayed coatings. Furthermore, research on the interactions of cells and tissues on sol-gel derived titanium oxide surfaces have shown promising results. It has been found that osteoblasts adhesion and matrix mineralization is significantly more on the coated surfaces. In addition, experiments in rats and dogs revealed less inflammation and direct attachment between soft-tissue components and sol-gel derived TiO_2 coatings (Areva et al., 2004; Paldan et al., 2008a; Wennerberg et al., 2011).

In contrast to the advances described previously, surface treatments solely focused on improving the attachment of soft tissues on implant surfaces have only recently gained attention in the literature. Furthermore, most of the conducted research utilize titanium. Despite the increasing use of zirconia in implant dentistry, only few studies have been done for optimizing zirconia surface in different biologic environments. In a recent study, Patel et. al. (2017) attempted at optimizing zirconia for biomedical applications by TiO_2 nanotubes. They showed that nanotubes on zirconia surface improve cell viability, attachment and elongation. However, a drawback of anodized titanium nanotubes on the surface of zirconia is the gray colored appearance that they induce. In another study, Zheng et. al. (2015) reported a higher fibroblast density and higher expression of cell attachment genes on zirconia that were modified by plasma treatment. Considering the lack of studies in this field, this project was initiated aiming at improving the zirconia surface properties for better soft-tissue/zirconia integration.

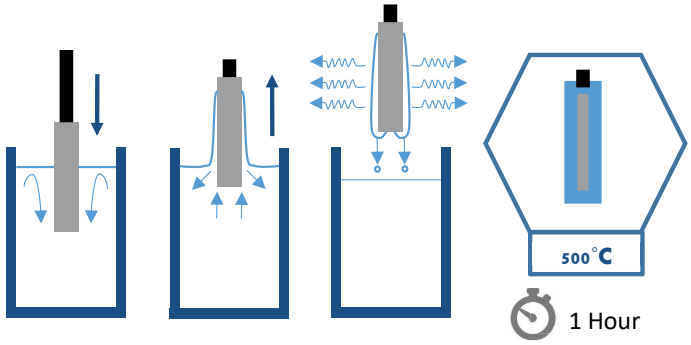

Figure 2 *Schematic diagram illustrating the sol-gel dip-coating method used in this thesis. Samples are inserted and withdrawn from a solution containing TiO_2 particles. The resultant coating is later on sintered at 500℃ for 1 hour.*

3. AIMS OF THE THESIS

The research presented here was based on the hypothesis that sol-gel derived titanium dioxide coatings on zirconia will improve its biocompatibility and attachment to the gingival tissues. Correspondingly, the following aims were set to:

1. Determine if the coating or the coating process weaken the mechanical strength of the zirconia (Study I).

2. Evaluate blood protein adsorption, blood thrombogenicity and platelet morphology on the coated surfaces (Study II).

3. Study the adhesion and proliferation of fibroblasts and epithelial cells on the surfaces *in vitro* (Study I and III).

4. Characterize the effect of surface treatment on wettability (Study III).

5. Examine the effect of coatings on the nature and strength of gingival tissue attachment on zirconia implant surface (Study IV).

4. MATERIALS AND METHODS

The roman numbers after each heading specify the study in which the described methodologies were used.

4.1. Specimen preparation

Specimens of different shapes were fabricated for each experiment separately. A surgical saw (Struers Secotom-50, Copenhagen, Denmark) was used to cut yttrium stabilized zirconia blocks (ZirkonZahn, Taufers, Italy) in the green stage. Each specimen was sequentially ground using silicon carbide grinding paper, finishing with FEPA #1200. (LaboPol 21, Struers A/S, Rodovre, Denmark). The specimens were sintered according to the manufacturer's instructions and were then cleansed using ultrasound in baths of acetone and ethanol for 5 minutes. In addition, readily manufactured zirconia endodontic posts (CeraPost®, Komet Dental, Gebr. Brasseler GmbH & Co., Lemgo, Germany) were used to function as implants in study IV.

Specimens used in blood response (II), cell culture (I, III) and tissue culture (IV) experiments were autoclaved for 20 minutes at 121ºC before use.

4.2. Sol-gel coatings

4.2.1. TiO_2 coating

Tetraisopropylorthotitanate [$Ti(OCH(CH_3)_2)_4$] was dissolved in 95% ethanol. Ethanol, nitric acid and ultrapure water were then mixed to yield a second solution. This solution was then added to the Tetraisopropylorthotitanate solution drop by drop and the resultant solution was stirred vigorously and was left to age at room temperature for 24 hours. This resultant solution was used to coat the specimens with TiO_2. The specimens were dipped into the solution and then withdrawn at a speed of 0.3mm/s. The coated specimens were finally heated at 500°C for 10 minutes and were again cleansed ultrasonically in baths of acetone and ethanol for 5 minutes.

4.2.2. ZrO_2 coating (I)

ZrO_2 nanocoatings were applied in the first study to evaluate their potential. Briefly, at first zirconium n-propoxide (70% n-propanol) was dissolved in acetylacetone. A second solution was made by mixing acetylacetone and ultrapure water. This solution was then added to the zirconium n-propoxide solution drop by drop and stirred vigorously. Polyeteylene glygol (PEG) was added to the solution to slow down solvent evaporation. To coat the specimens, the specimens were dipped into the final solution and withdrawn at a speed of 0.5mm/s. The coated specimens were then heat treated in an oven with a gradual increase in temperature; 0-300°C (30 minutes), 300°C (1 hour), 300-550°C (30 minutes) and 550°C (30 minutes). The specimens were cooled down for 4 hours and finally cleansed ultrasonically in baths of acetone and ethanol for 5 minutes.

4.3. Ultraviolet irradiation (II)

TiO_2 coated specimens were irradiated for 1 hour with ultraviolet radiation. The specimens were placed 20 cm under an ultraviolet-C lamp (wavelength 254 nm) (Puritec HNS S11W, Osram, Augsburg,

Germany). These parameters are known to have photocatalytic effect on titanium dioxide existing in anatase form (Fujishima et al., 2000).

4.4. Compressive strength measurements (I)

This test employed 45 discoid specimens. ISO Standard 6872 was used as a reference to determine the biaxial flexural strengths. All specimens were tested using a universal material testing machine (LRX/LRX5K, Lloyd Instruments, Fareham, England) at room temperature. A flat piston (diameter 1.6 mm) was used to apply a load (1.0 mm/min) to the center of each specimen until fracture occurred. Each specimen rested centrally on three symmetrically based balls (Figure 1). The results were recorded using Nexygen software (Lloyd Instruments, Fareham, UK) and the biaxial flexural strength was calculated as previously described by Sulaiman et al. (2015):

$$S = 0.2387P(X - Y)/d^2$$

S: biaxial flexural strength (MPa); P: fracture load (N); d: specimen disk thickness at fracture origin (mm).

$$X = (1 + v)\ln\left(\frac{B}{C}\right)^2 + [\frac{1 - V}{2}]\left(\frac{B}{C}\right)^2$$
$$Y = (1 + v)\ln\left(\frac{A}{C}\right)^2 + [\frac{1 - V}{2}]\left(\frac{A}{C}\right)^2$$

v: Poisson's coefficient (ceramic=0.25, ISO 6872); A: radius of support circle (mm); B: radius of loaded area (mm); C: radius of specimen disk (mm).

4.5. Surface roughness measurements (I, II)

An atomic force microscope (AFM) (NNTEGRA Prima, NT-MDT, Russia) was used to take images of the surfaces of the specimens. Images of size 5 μm by 5 μm were taken with a resolution of 1024 x 1024 pixels using a HQ:NSC14/Al BS cantilever (μmasch, Estonia) (T=24+/-1 C, RH%=37.5+/-2.5). The software Scanning Probe Image Processor (SPIP, Image Metrology, Denmark) was used to analyze the height profiles.

4.6. Surface wettability (III)

4.6.1. Contact angle measurements

A contact angle meter (Attension Theta, Biolin Scientific, Sweden) was used to measure contact angles (θC) using the sessile drop method, on square shaped specimens (10x10x2 mm). A video camera was used to record images of a drop deposited on the surface of the samples. The contact angles from the shape of the drop were calculated by the device's image analysis system using the Young-Laplace equation, yielding the contact angles on both sides of the droplet and their mean values. Three liquids were used as a probe for SFE calculations: diiodomethane, formamide and distilled water. Ten drops were analyzed with each liquid on each of the tested surface types.

4.6.2. Surface free energy calculations

The SFE was calculated using two theoretical models, the Owens-Wendt (OW) and Van-Oss (VO) approaches. The OW model approach gives the long-range dispersion (Lifshitz-van der Waals) (γd) and the short-range polar (hydrogen bonding) (γp) components of SFE, and the VO approach brings the dispersive (γLW) and the polar acid-base (γab) components, the latter divided into two parts, acidic (γ+) and basic (γ–) according to the following equations:

$$1 + cos\ \theta = 2(\gamma_s^d)^{1/2}\left(\frac{\left(\gamma_L^d\right)^{1/2}}{\gamma_L}\right) + 2\left(\gamma_s^p\right)^{1/2}\left(\frac{\left(\gamma_L^p\right)^{1/2}}{\gamma_L}\right)$$

$$(1 + cos\ \theta)_{\gamma L} = 2\left[(\gamma_s^{LW}\gamma_L^{LW})^{1/2} + (\gamma_L^-\gamma_s^+)^{1/2} + (\gamma_s^-\gamma_L^+)^{1/2}\right]$$

where γ_s is the SFE of the surface, γ_L the SFE of the liquid, and $\gamma_s^{ab} = (\gamma_S^-\gamma_L^+)^{1/2}$

For both methods, the spreading pressure was not considered. This pressure contributes to SFE and has to be considered if the SFE is higher than 60 mJ/m². In the present work, SFE values were lower than this limit and the spreading pressure can be disregarded.

4.7. Blood response (II)

4.7.1. Blood coagulation on surfaces (thrombogenicity)

A healthy non-smoking female volunteer who had not taken any medications at least for the past 10 days donated the blood used in the following set of experiments. The first 3 ml of the withdrawn blood was thrown away to avoid contamination with tissue thromboplastin. Each specimen (Square-shaped; 10x10x2 mm) (n=4/time-point) was left in wells of a 6-well plate and received 100 μl of the blood on its surface. The specimens were then incubated at room temperature for 10, 20, 30, 40, 50 and 60 minutes. After the incubation periods, 3 ml of ultrapure water was poured into the wells using a pipette to flood the specimens, resulting in a solution of water and dissolved blood. This resultant solution was sampled in triplicate (200 μl each) and transferred to a 96-well plate after 5 minutes. The addition of ultrapure water lyses any red blood cell that is not trapped in a thrombus, releasing their hemoglobin. The absorbance level of the solutions was measured using an ELISA plate reader at 570 nm, which correlates with the concentration of the released hemoglobin in the solution after the addition of ultrapure water. The size of the clot formed on the surfaces of the samples is inversely proportional to the absorbance value recorded.

4.7.2. Platelet morphology on surfaces

The whole blood collected from the volunteer was mixed with 0.109 M solution of sodium citrate at a ratio of 9:1 (blood/sodium citrate solution). This mixture was then centrifuged at 1500 rpm for 15 minutes at room temperature to isolate the platelet-rich plasma (PRP). 100 μl of the PRP collected was then placed on the surfaces (n=5) of the specimens (Square-shaped; 10x10x2 mm), which were then incubated for 1 hour at 37°C. After the incubation period, the specimens were washed off three times with phosphate buffered saline (PBS) to discard excess remnants of the PRP droplet placed. Adherent platelets were then fixed for 2 hours at room temperature with 2.5% glutaraldehyde and were then successively dehydrated at increasing alcohol concentrations (20%, 40%, 60%, 80%, 90% and 100% for 15 minutes each). All

dried specimens were mounted on a metal stub and were sputtered by 20nm of gold using a sputter coater (Temcarb TB500, Emscope Laboratories Ltd., Ashford, United Kingdom). The surfaces of the specimens were then examined using a scanning electron microscope (SEM) (Leo Gemini 1530; Zeiss, Oberkochen, Germany) to count and observe platelet morphologies.

4.7.3. Blood protein adsorption on surfaces

The adsorbed proteins on surfaces of specimens were collected following few modifications to the method previously described by Tanner et al. (2003). The specimens (Square-shaped; 10x10x2 mm) were placed in tubes containing human plasma that was diluted with PBS at a ratio of 1:4. The tubes containing the specimens and plasma were then rolled for 30 minutes at room temperature. The specimens were then removed and washed twice with PBS. Microbrushes (Quick-Stick, Dentsolv AB, Saltsjö-Boo, Sweden) were wetted with 4 µl of sodium dodecyl sulphate polyacrylamide gel electrophoresis (SDS-PAGE) buffer (1mM Na-phosphate buffer, 2% SDS, 0.003% bromophenolblue). Each of the top and bottom surfaces of the specimens were rubbed with two wet brushes and finally with one dry one. This process is intended to desorb the plasma proteins bound to the surfaces of the specimens. The tips of these microbrushes were then cut off and placed in an Eppendorf tube containing 20 µl of the buffer. The tubes containing the microbrushes were then heated in a boiling water bath for 7 minutes. The tubes were then perforated with a needle and placed in larger tubes and centrifuged for 2 minutes (Heareus PICO17, ThermoFisher Scientific, Waltham, USA) to collect the sample solutions. Samples of duplicate specimens (from each surface) were collected in the same tube. The protein solutions were analyzed by SDS-PAGE and silver staining with the use of gradient Mini-Protean TGX gels (4-12%; Bio-Rad laboratories, Berkeley, USA). An imaging system (ChemiDoc MP, Bio-Rad laboratories, Berkeley, USA) was used to examine and take images of the resultant gels. The same procedure was also repeated by rolling the specimens in a solution of 0.125 mg/ml bovine fibronectin (F4759 Sigma, Sigma-Aldrich, St. Louis, USA), in order to evaluate the adsorption of fibronectin on the surfaces.

4.8. Cell culture experiments

4.8.1. Epithelial cells culture (III)

Spontaneously immortalized human gingival keratinocytes were obtained from a human gingival biopsy sample (Mäkelä, Salo, & Larjava, 1998). The extracted keratinocytes were then mixed in keratinocyte-serum-free medium (Gibco®, Thermo Fisher, USA) and cultivated on the surface of the specimens (20000 cells/cm^2) for 1, 3, 6 and 24 hours (n=4/time point) at 37°C. After the completion of each time-point, the specimens were washed twice with PBS solution in order to separate the unattached cells. Consequently, they were placed in TE-buffer (10mmol/l Tris, 1mmol/l EDTA), and stored at -70 °C. The quantity of adhered cells was measured with quantitative DNA measurement. The frozen samples were melted and thereafter sonicated for 30 seconds in a bucket of ice to release the genomic DNA of the keratinocytes. Intercalating dye (PicoGreen dsDNA kitti, Molecular Probes Europe, Holland) was added to the samples. A sample (100 μl) of this solution was pipetted and added to a microtiter plate. The amount of DNA was defined by measuring the fluorescence of the samples using excitation at an emission wavelength of 490 and 535 nm (Biotek synergy HT) and comparing it to a standard curve.

The proliferation of keratinocytes on the surface of the specimens was evaluated at days 1, 3 and 7 of culture (25000 cells/cm^2). After the time periods, the specimens were treated with AlamarBlue™ (Thermo Fischer, USA) and incubated for three hours. After the incubation, a 200 μl sample was pipetted on a

microtiter plate. The absorbance of the samples was measured using the wavelength of 570nm and 595 nm (Multiskan EX, Themo Labsystems). The volume of the cells was calculated by correlating the absorbance values to a standard curve.

4.8.2. Light microscopy analysis (III)

The specimens were washed with PBS and fixed by placing them in a solution of glutaraldehyde and PBS for 5 minutes. After fixation, the samples were washed twice with PBS and serially dehydrated in an ethanol with increasing dehydration. The discs were cut (Exakt 300 Diamond Band Saw, EXAKT Technologies, Inc, USA) to the sections and examined with a light microscope, to see the approximate amount and figure of the cells.

4.8.3. Fibroblasts culture (I)

Proliferation of human gingival fibroblasts was determined using AlamarBlue™ assay (BioSource International, Camarillo, CA) in colorimetric format. Fibroblasts were cultured (20,000 cells/cm^2) on the specimens (Square-shaped; 10x10x2 mm) for 12 days. The specimens (n=4) were withdrawn from the culture at days 1, 4, 7 and 12, and then placed into sterile culture plates containing fresh culture medium with 10% assay reagent. After 3 hours of incubation, the absorbance values were read at 560 nm and 595 nm using an ELISA plate reader (Multiskan MS, Labsystems, Helsinki, Finland). Measured absorbances were used to calculate the reduction of assay reagent, and the cell proliferation rate were normalized in respect to the proliferation rate of the control at the first time-point, which was arbitrarily set to 100%. A linear relationship between the cell number and absorbance readings was established on tissue culture polystyrene specimens.

4.9. Tissue culture experiment (IV)

4.9.1. Implant preparation

Zirconia endodontic posts (CeraPost®, Komet Dental, Gebr. Brasseler GmbH & Co., Lemgo, Germany) were implanted in porcine gingival tissue. Each endodontic post was cut in half using a surgical saw to yield implantable materials with heights of 9 mm and diameters of 1.90±0.02 mm (n=40). The implants were cleansed for 5 minutes in baths of acetone and ethanol each.

4.9.2. Tissue culture

A 6mm biopsy punch (Stiefel Biopsy Punch; Stiefel Laboratorium GmbH, Offenbach am Main, Germany) was used to cut out full thickness gingival explants from mandibles of freshly slaughtered pigs. Explants were then rinsed with PBS supplemented with penicillin, streptomycin and amphotericin B. An 18-gauge needle was used to pierce the explants in the center, creating a wound in which the implants were inserted. Prior to this, each implant was autoclaved for 20 min at 121ºC. The tissue/implant specimens were then individually placed in an air/liquid interface on a stainless steel grid, in wells containing Eagle's minimum essential medium supplemented with antibiotics and essential amino acids (EMEM M-2279) (Sigma-Aldrich Chemie GmbH, Steinheim, Germany) supplemented with 10 % fetal bovine serum (FBS), 100 U/lg penicillin, streptomycin 100 lg/ml, and 200 mM L-glutamine (Gibco BRL, Life Technologies, Paisley, UK). The plates containing implanted gingival tissues were then incubated at 37ºC in a 5 % CO_2 environment and the culture medium was changed every 24 hours up to 7 and 14 days in culture. Gingival explants with no implants were also cultured to serve as baseline controls for

general tissue morphology (microscopic examinations) and dynamic mechanical analysis (DMA) measurements.

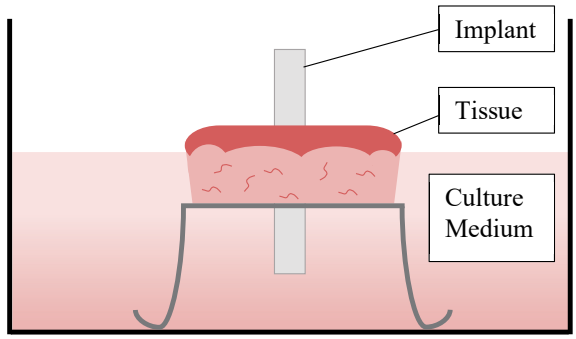

Figure 3 *Schematic view of the culture model. Tissue/implant specimen is suspended in the culture medium at an air/liquid interface (modified from Abdulmajeed et al. 2015).*

4.9.3. Embedding of tissue culture samples

A modification of the previously shown embedding method using Technovit 9100 New® polymerization system (Heraeus Gulzer GmbH, Wehrheim, Germany) was used (Bako et al., 2015; Willbold & Witte, 2010). Technovit 9100 New® is a technical resin based on polymethyl metacrylate (PMMA). It polymerizes in the absence of oxygen and at low temperatures (-2 to -20°C) and enables immunohistochemical staining for hard tissues. It is especially suitable for the studies of implant-tissue interface (Willbold & Witte, 2010). The embedding procedure involves four major steps; (i) fixation and dehydration, (ii) pre-infiltration, (iii) infiltration, and (iv) polymerization. Each of these steps require the use of different solutions (Figure 4).

To kick-off the process, 3-4 liters of Technovit 9100 New® base solution (stabilized base solution) was destabilized using a chromatography column containing 50g of Al_2O_3 (Sigma-Aldrich, St. Louis, MO, USA). Pre-infiltration solution 1 was made by mixing 200ml of xylene with 200ml stabilized base solution. Pre-infiltration solutions 2 and 3 were made by adding 1g of dibenzoylperoxide (hardener 1) to 200ml of the stabilized and destabilized base solutions, respectively. The infiltration solution was prepared first by adding 1g of hardener 1 to 200ml of the destabilized base solution. Then, 20mg of PMMA powder was mixed in the resultant solution to yield a homogeneous mixture, to which the destabilized base solution was added until the volume reached 250ml. For the stock solution A (for the polymerization step), 80g of PMMA powder was mixed in 400ml of the destabilized base solution, and while mixed rigorously, 3g of hardener 1 was added until a homogenous mixture was achieved. More destabilized base solution was added until the volume of the mixture reached 500ml. Stock solution B was prepared by mixing 30ml of destabilized base solution and 4ml of hardener 2 and then adding 2ml of regulator to the mixture while rigorously mixing. More destabilized base solution was added until the total volume reached 50ml. The final polymerization solution was made by mixing 45ml of stock solution A and 5ml of stock solution B. All the solutions were stored at -20°C.

After fixation, the specimens were washed for several hours with running tap water, and then dehydrated by placing them overnight in a series of alcohol and xylene at room temperature in the following steps; 70% alcohol, 96% alcohol, twice 100% alcohol, twice xylene. Following dehydration, the specimens were placed overnight in pre-infiltration solution 1 and then overnight in pre-infiltration solution 2, both at room temperature. Consequently, the samples were placed in pre-infiltration solution 3 and then in the infiltration solution, while incubated at +4°C overnight during both steps.

For polymerization of the tissue, 45 ml of stock A solution and 5 ml of stock B solution were carefully mixed. Each tissue sample was placed on the bottom of a precooled Teflon mold stored at +°4C with plastic forceps and the polymerization solution was added into the mold. Then, the tissue samples were placed in a vacuum desiccator cooled down to -4°C. The samples were evacuated at -4°C in 200-400mbar around 30 min or as long as any gas bubbles were detected. The pressure was let out of the vacuum desiccator and the molds were closed with their covers. The desiccator was closed and stored at -4°C for polymerization for 2 days. The hardened tissue blocks were pulled out of the molds and sent for sectioning.

4.9.4. Sectioning

The tissue blocks were first glued on plastic slides using Technovit 7210 VLC glue (Heraeus Gulzer GmbH, Wehrheim, Germany). The surface of the blocks was then ground using K400 and polished with K1000 diamond discs (Exakt Techologies, Oklahoma City, OK, USA). A second glass slide was roughened using a silicon carbide P500 paper (Exakt Techologies, Oklahoma City, OK, USA). The glass slide was washed in distilled water and the surface was cleaned with 100% alcohol and then one drop of RC Primer A (Heraeus Gulzer GmbH, Wehrheim, Germany) was put in the middle of the glass slide and the slide and was let to dry for 1 minute. Technovit 7210 VLC glue was placed on top of the dried primer and the glass slide was glued onto the tissue block-plastic slide complex using a gluing machine (Exakt Techologies, Oklahoma City, OK, USA) utilizing UV light for 15 minutes. The tissue block was hence sandwitched between two slides. Sample sandwich was clamped onto a diamond band saw (Exakt Techologies, Oklahoma City, OK, USA) and 100μm thick sections were cut. After that, the sections were ground using K400, K1000 diamond discs and then P1200, P2500 and P4000 silicon carbide papers (Exakt Techologies, Oklahoma City, OK, USA) until the thickness of 20 μm was achieved.

4.9.5. Immunohistological analysis

Before immunohistochemical staining, deplastination of the methyl methacrylate-embedded sections was performed. The slides were incubated twice in Xylene, twice in methoxy methyl acetate, twice in acetone and twice in distilled water. The sections were then rinsed by Phosphate Buffer Saline (PBS) and incubated in 0.05% trypsin for 15 minutes at room temperature. Sections were washed again in PBS, (3 times, 5 min each). This washing procedure was repeated between each step. After the wash in PBS, the sections were incubated at room temperature in a bath of 3% hydrogen peroxide for 30 minutes. Moving on, the PBS wash was repeated, and the sections were incubated at room temperature in 10% bovine serum albumin for 30 minutes. The sections were washed again with PBS and incubated overnight at 4°C in a 1:100 dilution of goat polyclonal IgG laminin γ2 antibody (C-20, sc-7652, Santa Cruz Biotechnology). PBS wash was repeated, and the sections were incubated at room temperature in a dilution of secondary antibody anti-goat (3 anti-goat :4 Dako dulitant) for 30 minutes, washed again in PBS and finally with diaminobenzidine (DAB). After the wash in PBS, the sections were counterstained

by placing them in hematoxylin for 1 minute at room temperature, dried, and covered with Pertex. All sections were analyzed under an Aristoplan photomicroscope (Leitz, Wetzlar, Germany) and the images were captured using a Leica DFC 320 digital camera (Leica Microsystems AG, Wetzlar, Germany) with Leica Application Suite version 4.1.0.

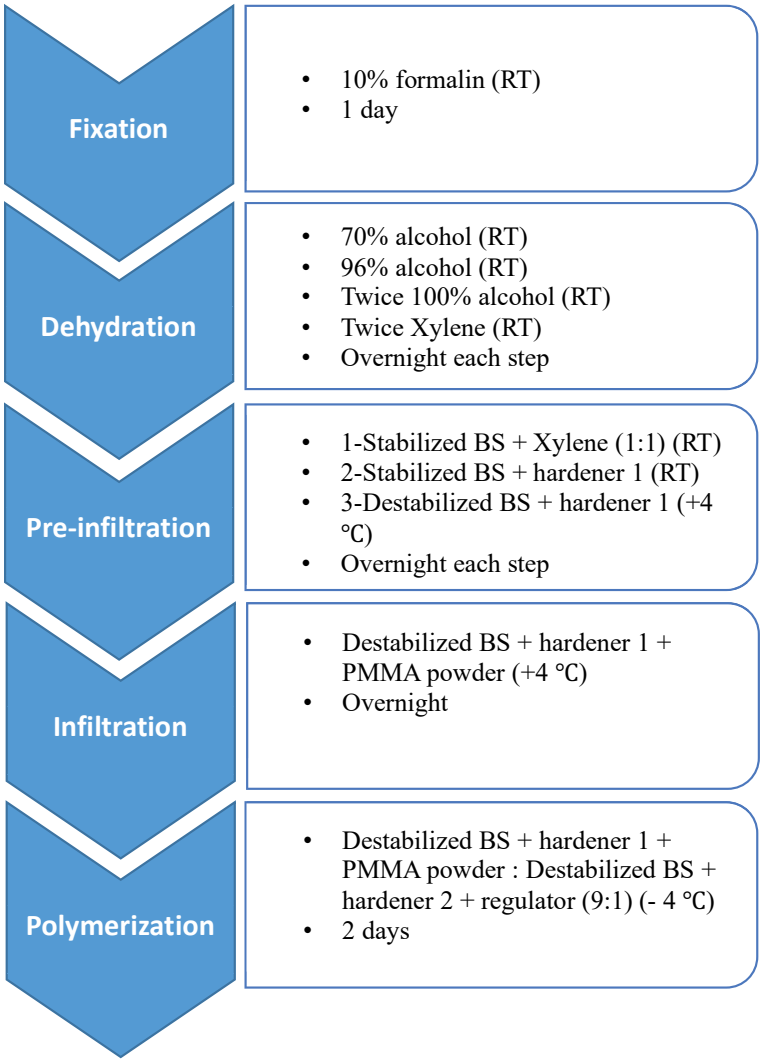

Figure 4 *Steps, solutions and incubation times used in study IV. A modification of the Technovit 9100 New ® embedding system. RT: Room temperature, BS: base solution.*

4.9.6. DMA – Dynamic Mechanical Analysis

The dynamic modulus and creeping modulus of the interface between the gingival tissue and the implants in shear mode were measured using a novel BEST (Biomaterials Enhanced Simulation Testing) protocol (Seqvera Ltd., Finland) in a dynamic mechanical analyzer (DMA 242E "Artemis", Netzsch Gerätebau GmbH, Germany). The specimens (i.e. gingival explants attached to the implants) were placed on the specimen holder of the analyzer. The setup applies oscillating sinusoidal force to the implants as shown in figure 5, straining them and creating displacement amplitude of 30μm. The forces were applied at a constant frequency of 1 Hz at 37°C, mimicking the cyclic masticatory rhythm and human body temperature (Lacoste-Ferré et al., 2011). For this specific setup and geometry, the geometric factor k_2 was experimentally determined as:

$$k_2 = 0.7386\left(1 - \left(\frac{r_a}{r_2}\right)^3\right)$$

where r_2 is the radius of the specimen holder, r_a is the radius of the implant.

Thus, the dynamic elastic modulus can be expressed as:

$$E_{dyn} = k_2 \frac{F_{dyn}\, r_2^2}{(h_0 + dL)^3 |A_s|}$$

and the tangential (creeping) elastic modulus as:

$$E_{stat} = k_2 \frac{F_{stat}\, r_2^2}{(h_0)^3 |dL|}$$

where F_{dyn} is the dynamic force amplitude on the specimen, F_{stat} is the static acting force, h_0 is the initial height of the tissue, dL is the change of the height during the measurement, and A_s is the displacement amplitude of a specimen. The dimensions of each specimen were measured using a laser micrometer (Metralight Co., California, USA) prior to their placement in the analyzer with a tolerance of ±1 μm.

For assessment of realistic stresses and displacements a 2D-axyisymmetric model was set up (COMSOL Multiphysics 5.3, Comsol Inc.) to estimate the distribution of the deformation inside the soft tissue attached to the implant, assuming the latter to be a rigid solid. This model was served as a visual guidance as exact properties of the soft tissue are not known in these conditions.

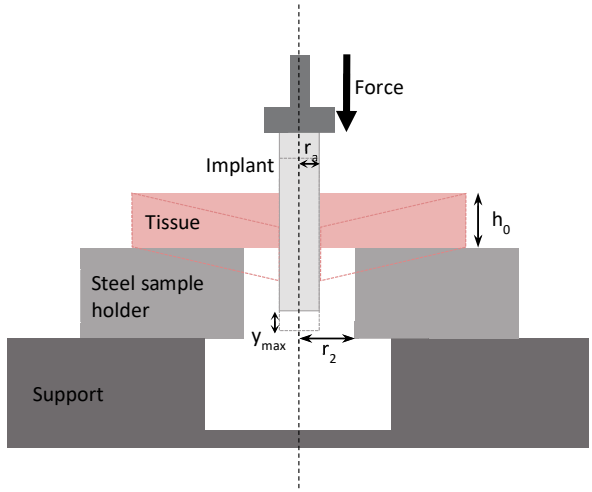

Figure 5 *Schematic view of the dynamic mechanical analysis test set-up. Tissue holding implants are supported on a holder and dynamic loads are exerted on the top of the implant creating distortion in the tissue.*

4.10. Scanning electron microscopy (I, II)

The specimens were mounted on a metal stub and sputtered by gold or carbon using a sputter coater (Bal-Tec SCD 050, Balzers, Liechtenstein). The surfaces of the specimens were then analyzed through images taken using a scanning electron microscope (SEM) (Model JSM 5500, Jeol Ltd, Tokyo, Japan) (Leo Gemini 1530; Zeiss, Oberkochen, Germany).

4.11. Statistical Analysis

Statistical analysis was performed with Statistical Package for the Social Sciences (Version 23.0, SPSS Inc., Chicago, Il, USA).

In study I, the data was analyzed using a one-way analysis of variance (ANOVA). Subsequent comparisons between different groups were performed with Tukey's post-hoc test. Differences were considered significant at 95% confidence level. In addition, the biaxial flexural strength data was also statistically analyzed with the Weibull distribution. The following equation was used to calculate the Weibull modulus :

$$P_{F(\sigma c)} = 1 - e^{[-(\sigma_c/\sigma_0)^m]}$$

$P_{F(\sigma c)}$: the probability of failure; σ_c : the fracture strength; σ_0: the characteristic strength ($P_{F(\sigma c)}$= 63.2%) and m: the Weibull modulus.

In study II, repeated measures analysis of variance (ANOVA) was used as the statistical test for the comparison of the absorbance means obtained from the blood coagulation study. Pairwise comparisons among the means were made using simple contrasts with Bonferroni corrected p-values.

In study III, differences in contact angles between groups were analyzed with the Student's t-test. All the cell culture data was examined with JMP Pro 12. The data did not correspond to the normal distribution in every time point, so it was analyzed using the Wilcoxon rank sum test. Differences between the groups were estimated to be significant at 95 % confidence level.

5. RESULTS

The roman numbers after each heading specifies the results pertaining to the study performed.

5.1. Compressive strength (I)

The calculated biaxial flexural strengths of non-coated zirconia and zirconia coated with either of TiO_2 or ZrO_2 are represented (Figure 6). No statistical significance was found between the biaxial flexural strengths of the groups (p=0.273).

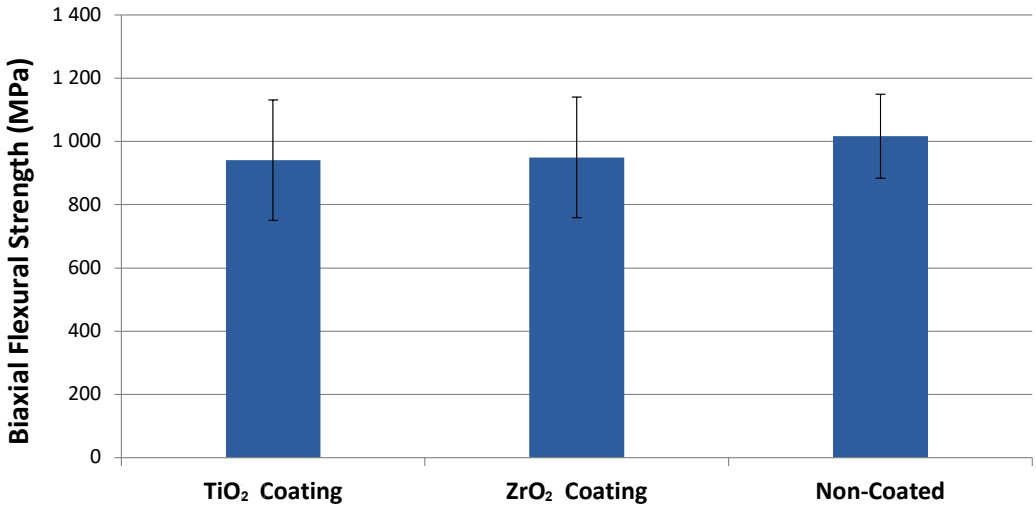

Figure 6 *Biaxial flexural strength (MPa) of the investigated groups (No significant difference, p=0.273).*

When comparing the Weibull moduli however, (Figure 7, Table 1) both the coated groups (5.4 and 5.7, for TiO_2 and ZrO_2 respectively) had lower values than the non-coated control group (8.0).

Coating	Weibull characteristic Strength (MPa)	Weibull modulus	Correlation co-efficient	5% Probability of Fracture (MPa)
TiO_2	993	5.7	0.968	585
ZrO_2	1010	5.4	0.970	588
Non-coated	1077	8.0	0.920	744

Table 1 *The Weibull modulus calculated in different groups.*

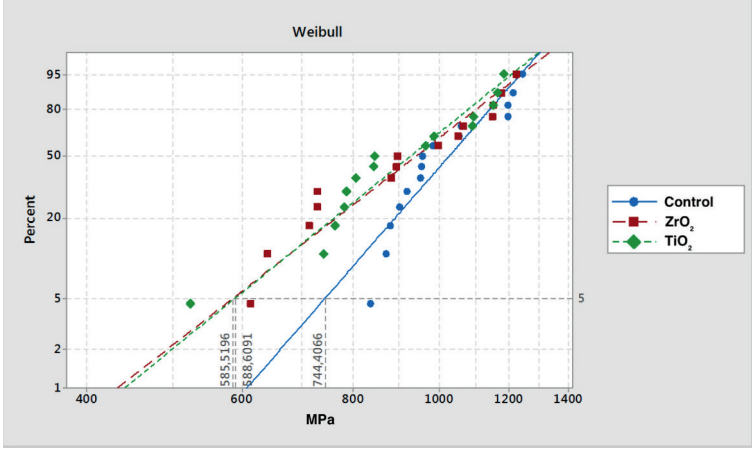

Figure 7 *The probability plot of fracture of specimens in different groups using Weibull distribution. Forces needed to fracture 5% of specimens in each group are recorded.*

5.2. Surface characteristics (I, II)

Surface characteristics of non-coated zirconia and zirconia coated with either of TiO_2 or ZrO_2 was evaluated. Images taken using atomic force microscopy revealed that TiO_2 coated specimens had a lower mean surface roughness (Sa) of 34.2 nm, than those with ZrO_2 coating, Sa 46.6 nm. Z heights were found to be 267 nm and 512 nm for TiO_2 coated group and ZrO_2 coated group respectively. The control non-coated group had a mean surface roughness (Sa) of 533.8 nm and Z height of 372.5 nm. The particles were well distributed and organized in all the groups (Figure 8). Furthermore, sol-gel coating on zirconia surface appears to have a smoothening effect. (Figure 8B).

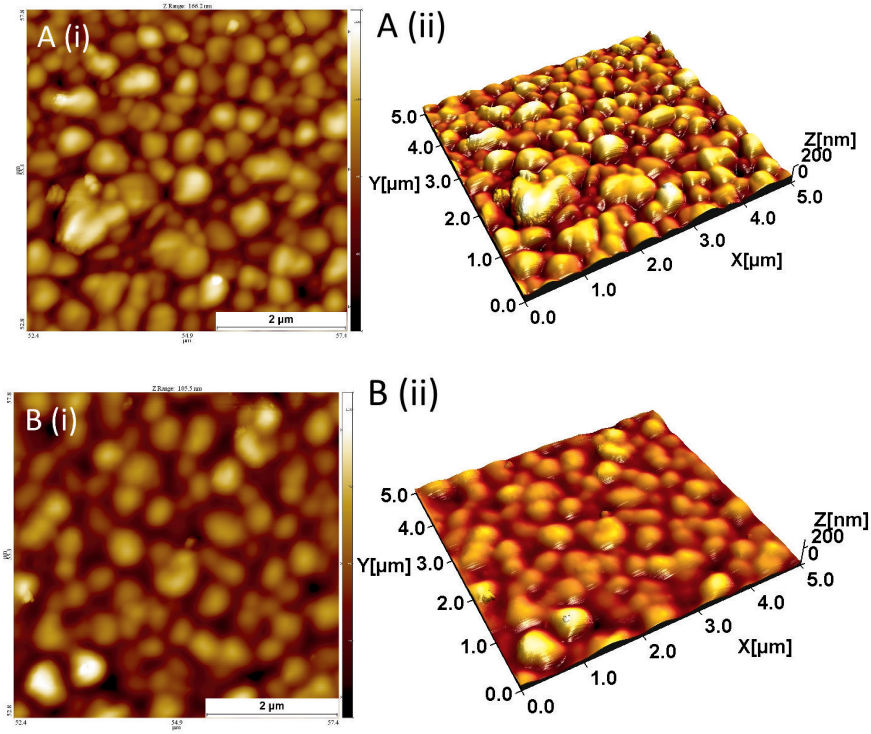

Figure 8 *The atomic force microscope images (AFM) of: (A) Non-coated zirconia, (B) TiO_2 coated zirconia. (i) Two-dimensional (2D) AFM image, (ii) Three dimensional (3D) AFM image.*

SEM images revealed smooth surface on TiO_2 and ZrO_2 coated specimens. However, cracks were apparent in high magnification on both coatings around surface irregularities of the substrates. No delamination of the coating was noticed. The granular structure of zirconia in addition to the presence of polishing linear grooves were visible on the SEM images of the control non-coated specimens (Figure 9).

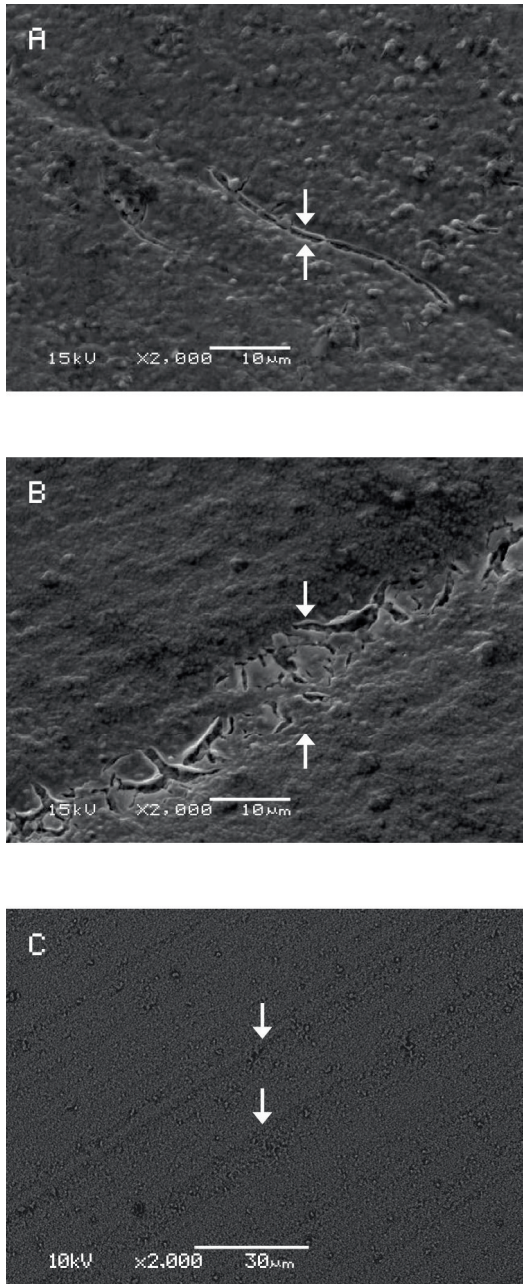

Figure 9 *Scanning electron microscope images of: (A) TiO_2coated, arrows indicating cracks on the coating. (B) ZrO_2 coated, arrows indicating cracks on the coating. (C) Control (non-coated), arrows indicating polishing grooves.*

5.3. Surface wettability (III)

Surface wettability experiments were conducted to compare non-coated zirconia and zirconia coated with TiO_2

5.3.1. Contact angle

Table 2 summarizes the contact angles obtained by the sessile drop method on the different surfaces. The contact angles for water and di-iodomethane were significantly lower on the coated specimens (* $p<0.05$).

					Contact angles (θC)	
Liquid	γtot [mN/m]	γd [mN/m]	γ+ [mN/m]	γ- [mN/m]	Non-coated Zirconia	TiO_2 Coated Zirconia
Di-iodomethane	50.8	50.8	0.0	0.0	42.5±4.6	37.3±4.2*
Water	72.8	21.8	25.5	25.5	74.1±6.9	53.0±4.8 *
Formamide	58	39	2.28	39.6	47.9±7.7	40.7±6.0

Table 2 *Test liquids and their surface tension components plus the mean values and standard deviations of contact angle measurements on TiO_2 coated and non-coated zirconia.*

5.3.2. Surface free energy

The different components of SFE are expressed in Figures 10A and 10B. Histograms are drawn for an easier comparison of the results. The total surface free energy calculated by the OW method is higher with the coated samples. Since the dispersive SFE calculated by this method are almost exactly the same for both the test groups (Figure 10B), the differences may be attributed to the polar component of the SFE that is higher for the coated samples as represented by both OW and Van-Oss calculations.

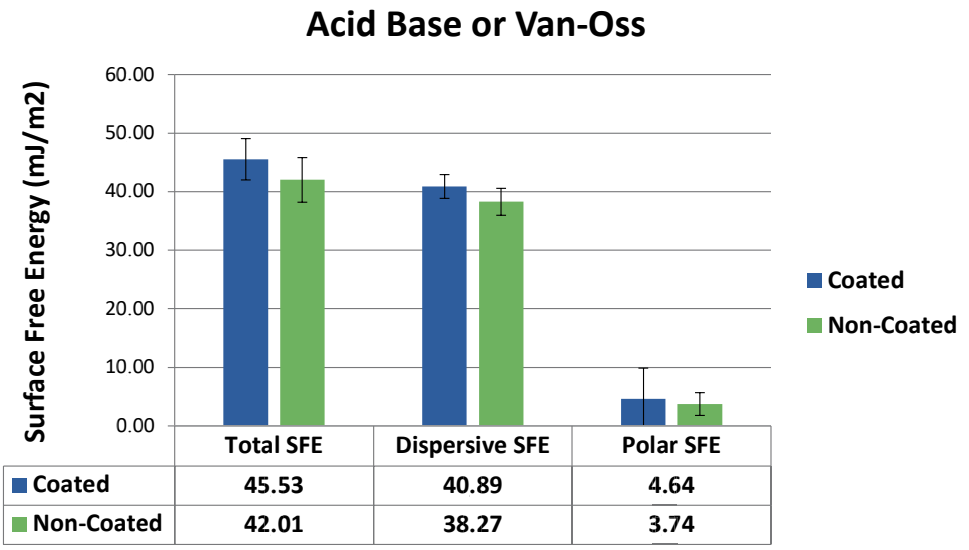

Figure 10A *Dispersive (γ^{D}), polar (γ^{P}), and total (γ^{TOT}) components of surface free energy calculated using the Van Oss approach*

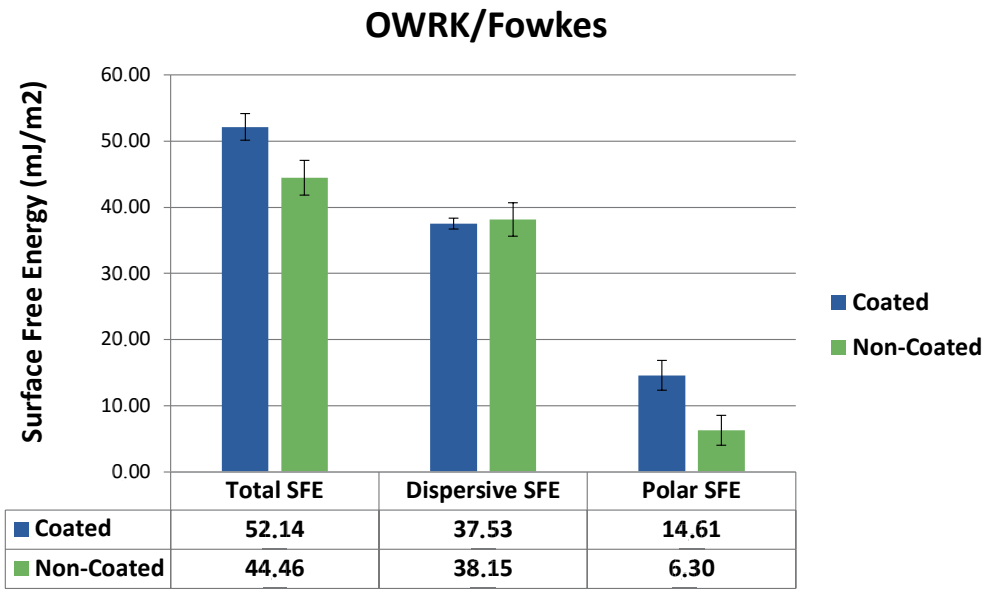

Figure 10B *Dispersive (γ^{D}), polar (γ^{P}), and total (γ^{TOT}) components of surface free energy calculated using the Owens-Wendt approach*

5.4. Blood response (II)

Blood response experiments were conducted to compare non-coated zirconia and zirconia coated with TiO_2. In addition, the coated experiments were irradiated with UV to see possible effects on their behavior.

5.4.1. Thrombogenicity

Figure 11 represents the blood-clotting profiles for the different groups. Both the coated groups, i.e. TiO_2 coated, in addition to the ones treated with UV irradiation, showed faster blood coagulation. Significantly lower ($p<0.005$) absorbance values were already recorded with the coated specimens at the 20-minute time-point. This reflects a higher amount of blood clotting. Similarly, the same differences were also present at the 30-, 40- and 50-minute time-points. Moreover, coated specimens that were treated with UV represented the highest extent of blood clotting at all the forenamed time-points ($p<0.005$). Blood is considered to have clotted completely when the optical densities drop below 0.3. The time taken for blood coagulation, in other words the total clotting time, was almost 30 minutes for the coated and UV treated specimens followed by 40 minutes and 50 minutes for the TiO_2 coated and non-coated control specimens, respectively. Moreover, statistically significant differences were also observed between the time points, stating that blood coagulation was more profound with the passage of time. ($p<0.001$) (Figure 11).

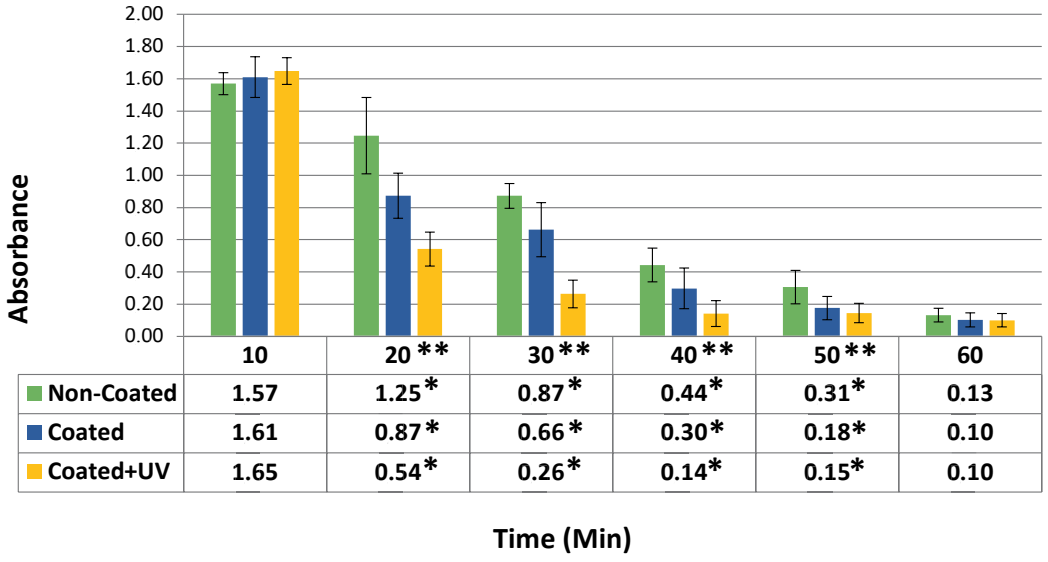

	10	20 **	30 **	40 **	50 **	60
Non-Coated	1.57	1.25*	0.87*	0.44*	0.31*	0.13
Coated	1.61	0.87*	0.66*	0.30*	0.18*	0.10
Coated+UV	1.65	0.54*	0.26*	0.14*	0.15*	0.10

Figure 11 *Blood-clotting profiles for non-coated, TiO_2 coated and UV irradiated TiO_2 coated zirconia. The plot shows the optical density vs time. Data are presented as mean values ± standard deviation. Table below the chart represents the respective absorbance values at each time-point.*
**Statistically significant differences between the groups at the marked time points ($p<0.005$). ** Statistically significant differences between the time points. ($p<0.001$)*

5.4.2. Platelet morphology

Figure 12 shows the platelet morphology after the 1-hour adhesion period. Panoramic images of the surfaces were taken. Each figure (Figure 12(i)) represents 30 stitched images of the surface at x2500 magnification. All groups showed platelet adhesion, however, with different platelet morphologies. The platelets on the TiO_2 coated specimens were more spread, more dendritic, more aggregated and therefore more active compared to the ones observed on the control, non-coated specimens. On the other hand, the platelets on the surface of the coated and UV treated specimens were discoid or round, which translates to a lower state of activation.

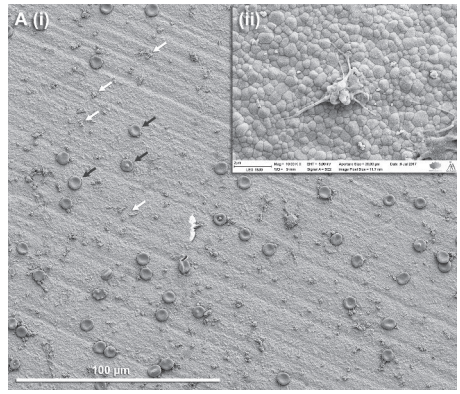

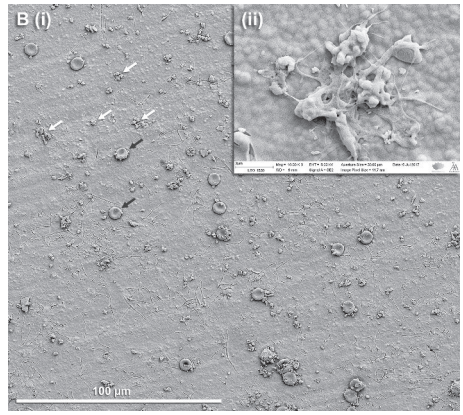

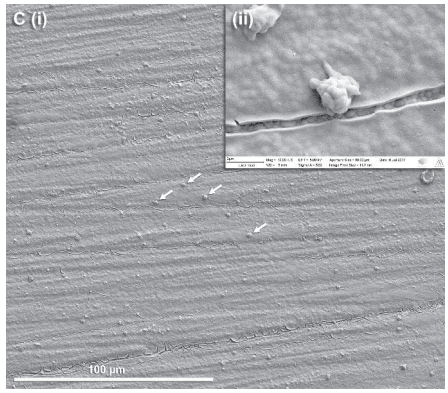

Figure 12 *Scanning electron micrographs of platelet morphologies after 1-hour adhesion period on (i) Panogramic image of 30 stitched images of the surface wetted with platelet rich plasma (PRP) at x2500 magnification. (ii) x10000 magnification of platelet morphologies. (A) non-coated zirconia, (B) zirconia coated with TiO_2, (C) zirconia coated with TiO_2 irradiated with ultraviolet radiation. NB. White arrows show platelets, black arrows show red blood cells.*

5.4.3. Blood protein adsorption

Albumin was adsorbed abundantly on the surfaces of all the specimens. All the surfaces adsorbed a broad range of plasma proteins and no consistent differences in the protein profiles were noticed. The amount of fibronectin adsorbed on the surfaces was also not different between the three groups (Figure 13).

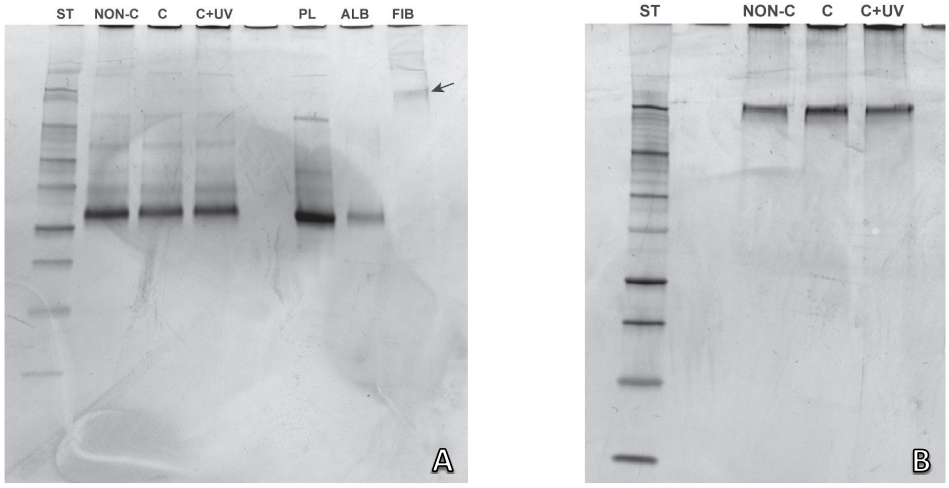

Figure 13 *Gel electrophoresis for (A) plasma proteins and (B) fibronectin adsorbed on the different test materials; NON-C: non-coated zirconia, C: zirconia coated with TiO_2, C+UV: zirconia coated with TiO_2 irradiated with ultraviolet radiation. Black arrow in figure 3A represents the band identifying fibrinogen. The protein standard contained proteins with the following molecular weights, in kD: 250, 150, 100, 75, 50, 37, 25, 20, 15, 10. Plasma: PL; albumin: ALB; fibrinogen: FIB.*

5.5. Cell culture (I, III)

5.5.1. Epithelial cells (III)

Epithelial cells were cultured on non-coated zirconia and zirconia coated with TiO_2. The number of adherent epithelial cells significantly increased between 1 and 3 hours of culture on both coated and non-coated specimens. During the first 6 hours, no differences were observed between the coated and non-coated specimens. However, later on, the coated samples showed a statistically higher increase in the number of epithelial cells between 6 and 24 hours compared to the non-coated ones, with the number of adherent cells being significantly higher at the 24-hour time-point ($p<0.05$) (Figure 14).

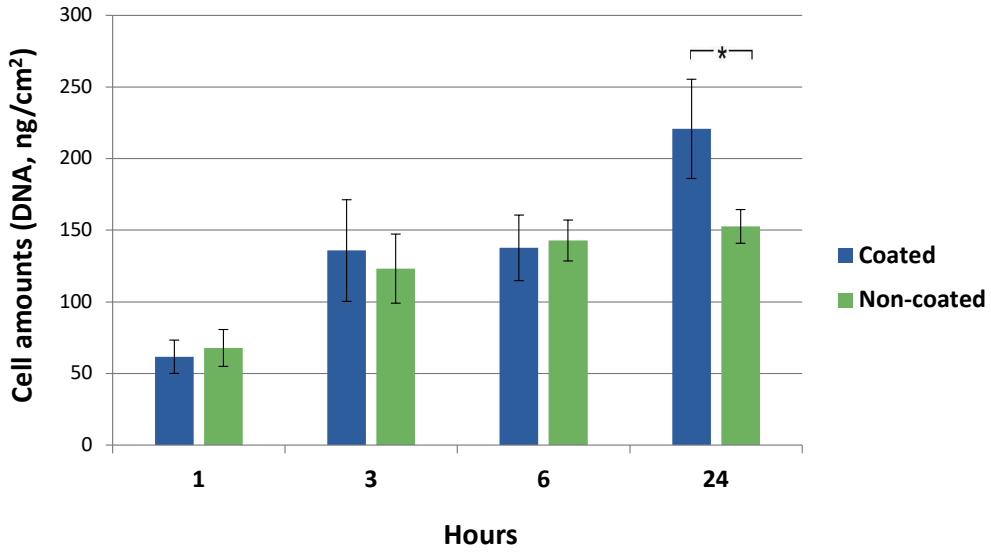

Figure 14 *Cell amounts (DNA, ng/cm²) after 1, 3, 6 and 24 hours of cell culture. Amounts are represented as mean ± standard deviation.*

The increase in the number of cells was continuous and significant in both the groups for the whole seven days. At every time-point, the number of epithelial cells was significantly more on the coated specimens. ($p<0.05$) (Figure 15).

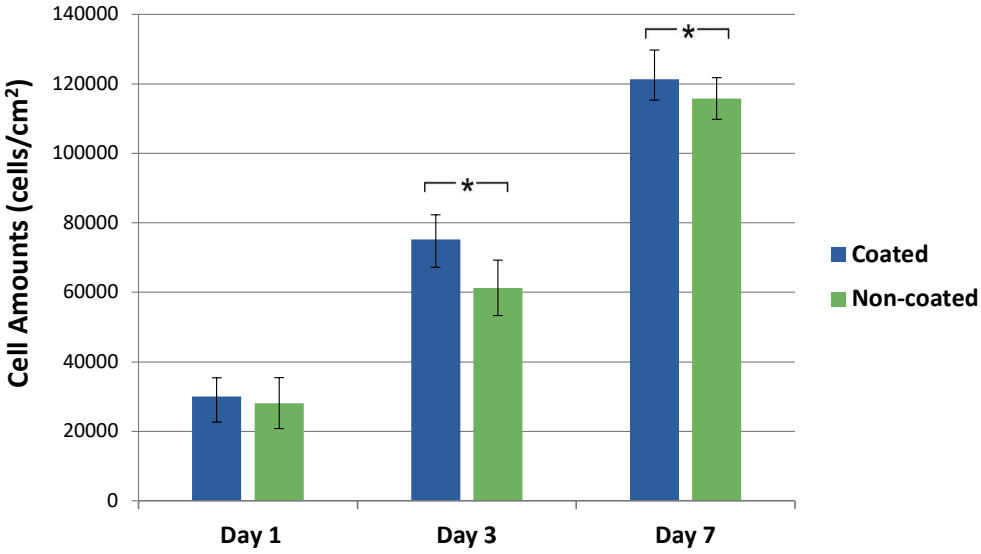

Figure 15 *Cell amounts (cells/cm²) after 1, 3 and 7 days. Amounts are represented as mean ± standard deviation.*

Light microscopy images revealed a higher number of cells and more uniform cell layers on the coated specimens than on the non-coated ones. The cells appeared viable with well-distinguished nuclei and cytoplasm. In addition, the cells seemed well elongated, which tells that the cells had certainly been attached to the surface. The gap appearing in the picture between the specimens and the cells is an artifact of the specimen processing for light microscopy (Figure 16).

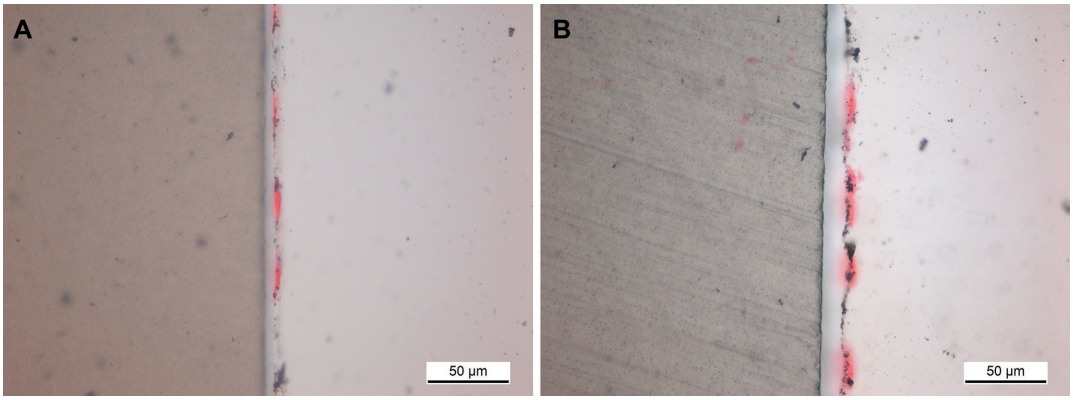

Figure 16 *Light microscope images of (A) TiO_2 coated, (B) non-coated zirconia samples. TiO_2 coated samples show more adherent cells with a more uniform cell layer. The gaps between samples and cells is considered to be a cutting artifact.*

5.5.2. Fibroblasts (I)

Fibroblast proliferation was tested on non-coated zirconia and zirconia coated with either of TiO_2 or ZrO_2. Fibroblast proliferation on all groups increased consistently with the increasing culture time with no significant difference among the groups at day 7. At day 1, cell proliferation was significantly higher ($p<0.05$) on TiO_2 coatings compared to ZrO_2 and the control group. However, at day 4, the control non-coated specimens showed higher cell proliferation ($p<0.05$). The highest proliferation activity was observed on day 12 where ZrO_2 coatings had significantly lower cell proliferation ($p<0.05$) compared to the other groups. Figure 17 illustrates the mean reduction of the AlamarBlue™ assay by each test group, presented as a percentage, which corresponds to the activity of proliferating fibroblasts.

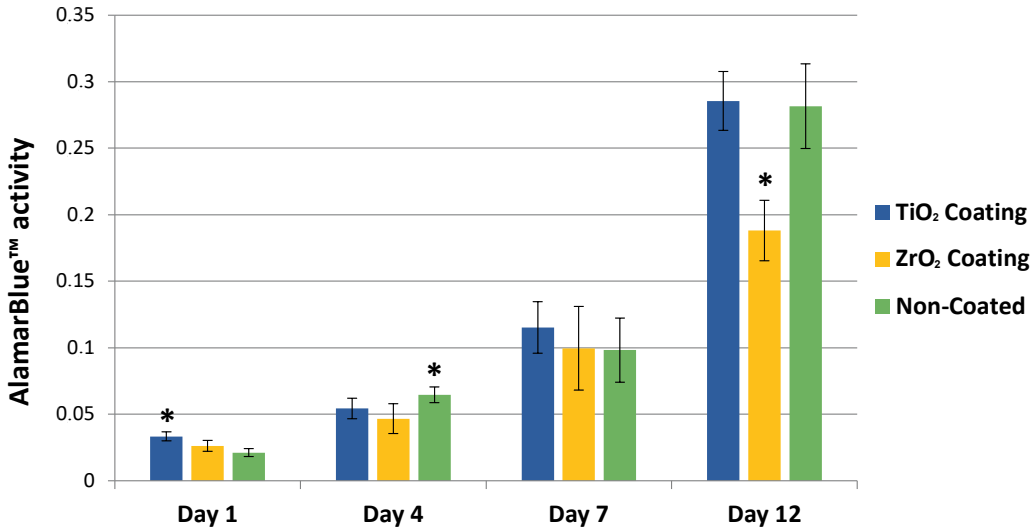

Figure 17 *Proliferation of human gingival fibroblasts on different groups. The reduction of AlamarBlueTM reagent with control specimens at day 1 time-point was set to 100%. Data are presented as mean ± standard deviation (n=4) *significantly different.*

5.6. Tissue culture (IV)

5.6.1. Immunohistochemistry

As a positive control, Laminin γ-2 -chain appeared as an immunoreactive band in the basement membrane zone of the porcine gingival tissue cultured in vitro (Figure 18 A). The epithelial cells of the gingival explants were seen to have migrated in order to cover the exposed connective tissue, proving that the explants were vital throughout the culture period (data not shown). In the sections harvested at the 7 days of culture, tissue in contact with the coated implants appeared to be more firmly attached to the implant surface (Figure 18B) compared to non-coated implants (Figure 18C). Laminin γ-2 -chain stained positively in the most apical cells of the epithelium in contact with the implant surface and also clearly in the basement membrane facing the connective tissue close to the implant (Figure 18B). There was not any clear staining of laminin γ-2 -chain detected at the contact of epithelium with non-coated zirconia at day 7 (Figure 18C). Sections from day 14 of culture also revealed a firm attachment of epithelium and connective tissue to the coated implant surfaces (Figure 18D, E, F). Laminin γ-2 -chain was present in the contact of the epithelium with the implant more extensively (Figure 18 D, E). Although sloughing of gingival epithelial cells appeared (a phenomenon that happens in the epithelium of all tissue explants), the attachment of the epithelium to the coated implants seemed to be firm and unaffected (Figure 18F). There was also positive staining of laminin γ-2 –chain at the epithelium-non-coated zirconia implant interface, but not as clearly as with the coated implants (Figure 18G). Moreover, the tissue appears to be more weakly bonded and detached from the implant surface. In both non-coated and coated zirconia implants, the epithelium did not show apical migration between the explant and the implant surface, which allows maturation of connective tissue attachment.

Figure 18 *Light microscopy images of porcine gingival tissue and implant/tissue complexes cultured in vitro. E: epithelium, CT: connective tissue.*

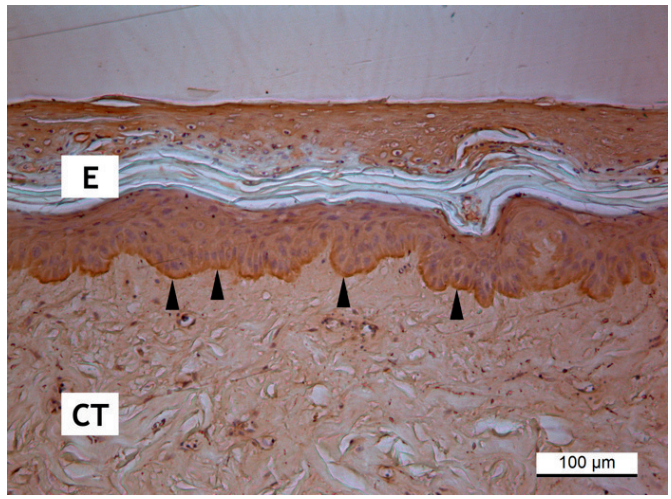

(A) *Gingival tissue cultured at the air-liquid interface for 7 days and stained with laminin γ-2 -chain antibody specific for laminin-332. A clear staining can be detected at the basement membrane zone between the epithelium and the connective tissue (black arrow heads). The superficial layers of gingival epithelium are sloughing off from the basal compartment of the epithelium, which is a phenomenon seen in all tissue cultures included the study.*

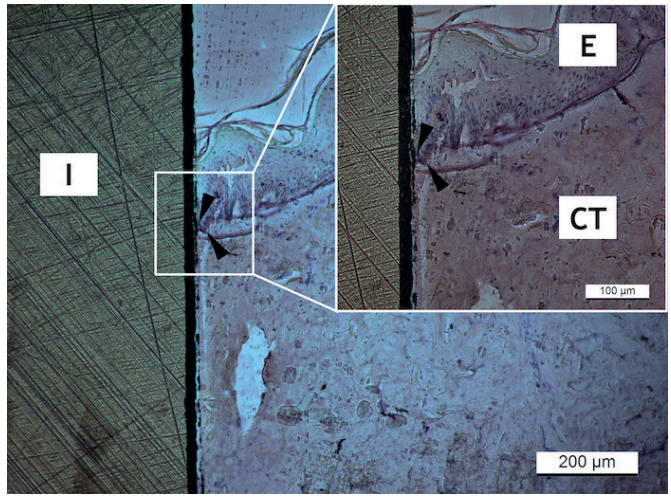

(B) *A coated implant/tissue complex at day 7 of culture. Both the epithelium and connective tissue are firmly attached to the TiO_2 coated implant surface. Laminin γ-2 -chain can be detected along the junction of the epithelium with the implant surface (top black arrow head). The most obvious staining can be detected at the most apical (closest to connective tissue) part of the epithelium facing the implant surface and at the basement membrane facing the gingival connective tissue close to the implant surface (bottom black arrow head).*

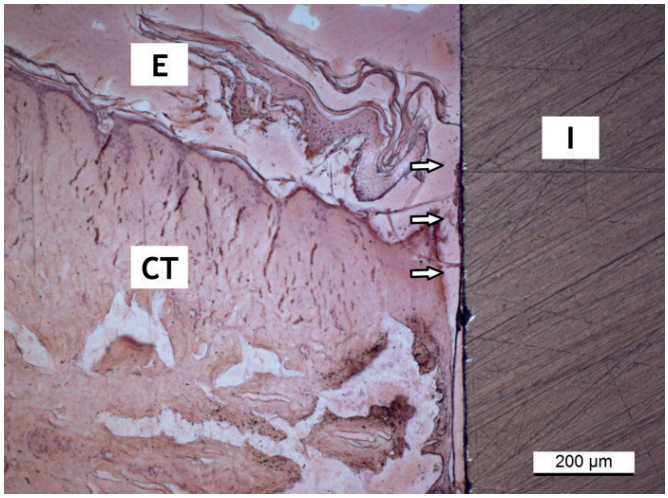

(C) *A non-coated implant/tissue complex at day 7 of culture. Laminin-γ-2 –chain can not be detected at the implant-epithelium interface. Epithelial tissue and connective tissue are detached from the implant surface (white arrows).*

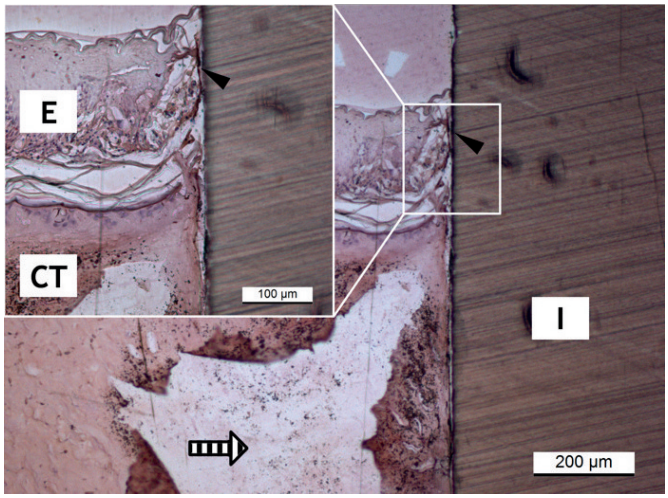

(D) *A coated implant/tissue complex at day 14 of culture. Laminin γ-2 –chain is expressed along the junction of the epithelium with the coated implant surface (black arrow heads). Despite rupturing within the connective tissue (striped arrow), the tissue is firmly attached to the implant surface.*

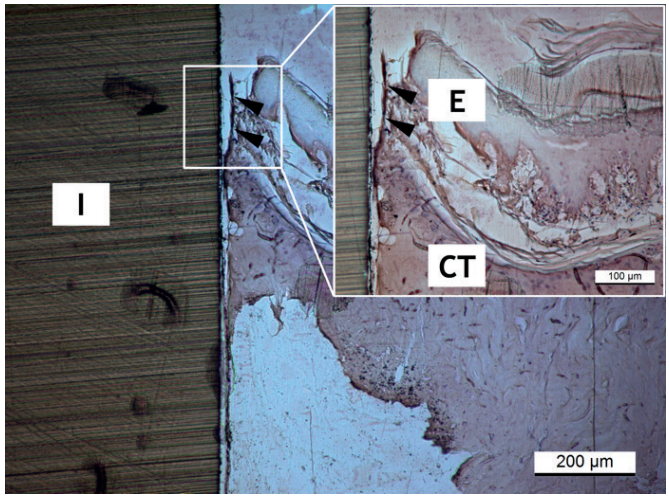

(E) *A coated implant/tissue complex at day 14 of culture. Laminin γ-2 –chain is strongly expressed along the junction of the epithelium with the coated implant surface (black arrow heads). Also, the epithelium extends further apically along the implant surface indicating maturation of the peri-implant epithelium.*

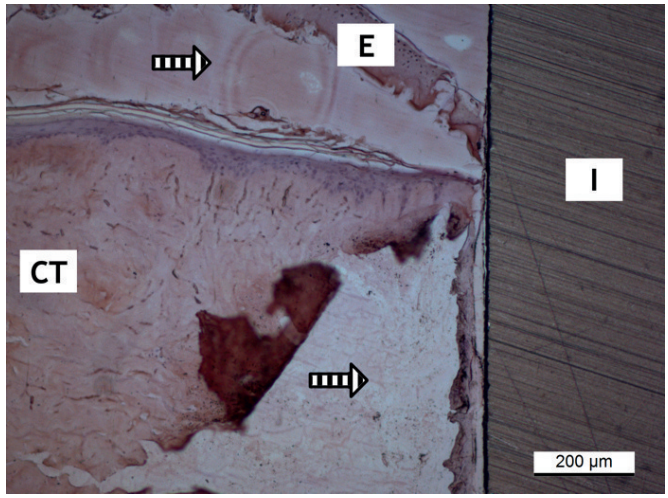

(F) *A coated implant/tissue complex at day 14 of culture. Despite sloughing of the uppermost epithelial cell layers (top striped arrow) the attachment of the epithelial cells to the implant surface seems to be very strong. Also, connective tissue is in close contact to the implant surface. The rupturing of connective tissue (bottom striped arrow) in these in vitro samples happens few micrometers away from the connective tissue-implant interface.*

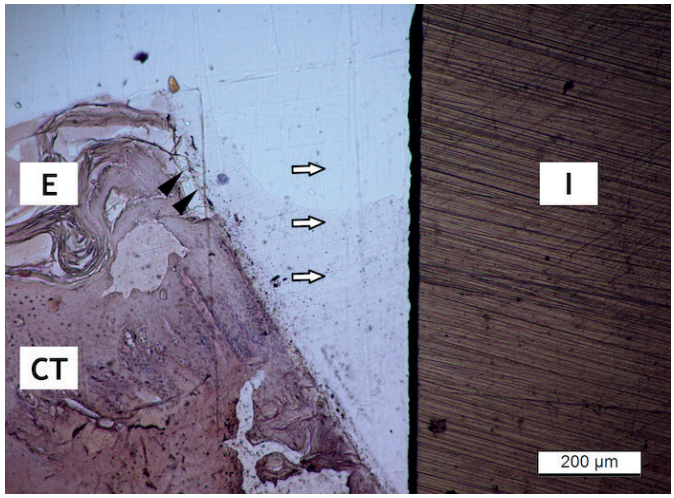

(G) *A non-coated implant/tissue complex at day 14 of culture. Laminin γ-2 –chain is weakly expressed at the epithelial cells facing the implant surface (black arrows). Epithelial and connective tissues are separated from the implant surface (white arrows).*

5.6.2. Dynamic mechanical analysis

Figure 19A displays the dynamic elastic modulus of the coated and non-coated implanted zirconia compared, at both days 7 and 14 of culture. Coated zirconia specimens showed substantially higher dynamic modulus compared to non-coated control at both days 7 (+88% vs. control) and 14 (+109%) (Figure 19A). Similarly, under creeping conditions (pseudo-static) the modulus of adhesion was also improved for the coated specimens at both days 7 (+5%) and 14 (+55%) (Figure 19B).

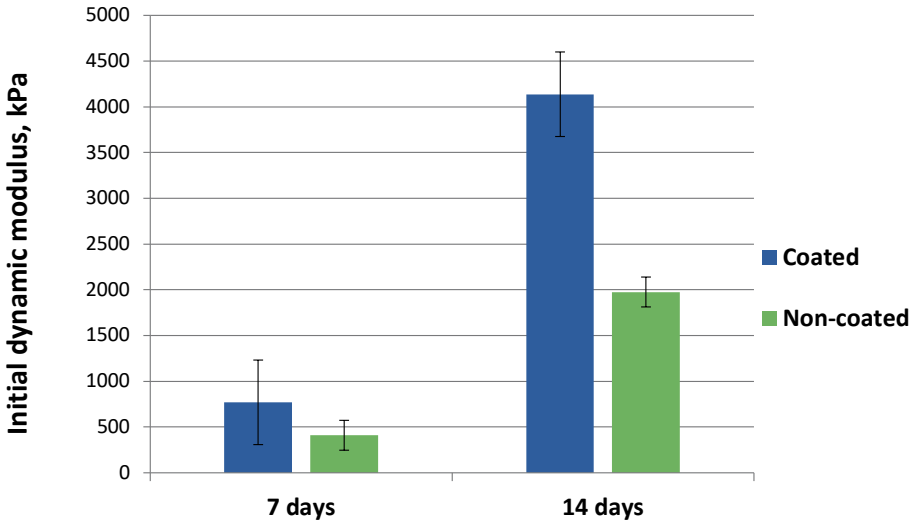

Figure 19A *Initial dynamic modulus of the tissue attachment apparatus calculated in both test groups at day 7 and 14 of culture.*

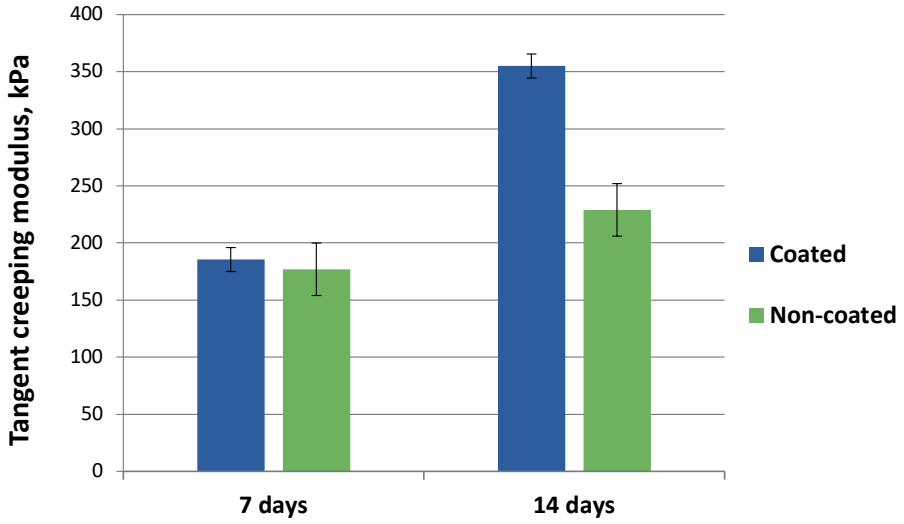

Figure 19B *Tangent creep modulus of the tissue attachment apparatus calculated in both test groups at day 7 and 14 of culture.*

6. DISCUSSION

6.1. General discussion

The aims of the performed series of *in vitro* studies was to utilize sol-gel derived TiO_2 coatings to improve the surface properties of zirconia in terms of better soft-tissue adhesion. Zirconia has gained popularity in dentistry in the recent years and has also found its path into permucosal applications like implant abutments or copings for indirect restorations. The design of this series of studies was based on the lack of data on the biological properties of zirconia in general, and towards improving these properties. The mechanical properties of the coated zirconia, the thrombogenicity, cytocompatibility, surface wettability, as well as nature and the strength of gingival tissue attachment on the zirconia surface were evaluated. The clinical significance, when possible, was an important aspect of the design and the methodologies used in the studies.

The mechanical properties of zirconia have been investigated intensively. In the first study the effect of the coatings and the coating process on the mechanical properties of zirconia were investigated through evaluation of biaxial flexural strengths. Since it was found that the coatings did not weaken fracture strength of zirconia, further steps were taken to evaluate the nature of this yielded material with blood and gingival tissues. Initially, coatings of ZrO_2 were also investigated, but these coatings demonstrated poor fibroblast cell proliferation; a test that serves as a baseline for primary prediction of soft tissue attachment (Kageyama et al., 1994), and were therefore excluded from the remaining studies.

Blood is the first tissue that comes into contact with any biomaterial that is placed in the body. This is also true during the surgical placement of dental implants were a wound is created. This wound has to favorably trigger inflammatory processes that will lead to the process of wound healing and eventual acceptance or rejection of the biomaterial placed. To understand this and to predict the clinical outcomes, the initial reaction of blood to the coated zirconia was evaluated. Furthermore, the behavior of platelets and the adsorption of different blood proteins on coated and non-coated zirconia surfaces were observed. In addition to a faster blood coagulation *in vitro,* coated zirconia specimens also had platelets at a higher activation state, which all can translate to a faster wound closure and healing clinically.

The junctional epithelium that is in contact with teeth or implant abutments is composed of both epithelial and connective tissues. The epithelial component is composed of gingival epithelial cells and the connective tissue is mainly composed of fibroblasts and collagen fibers. The proliferation of both these cell types were evaluated and the coated specimens demonstrated better results with higher epithelial cell adhesion and proliferation. These tests can initially predict the overall reaction of the material with soft tissues, however, testing the material with real gingival tissues and subsequently with actual human subjects is still necessary to draw definitive conclusions. Simultaneous with these cytocompatibility tests, the surfaces of coated and non-coated zirconia were also evaluated in terms of surface characteristics and wettability to confirm the findings. Surface wettability and free energy are considered to be important parameters in adhesion, morphological change and proliferation of cells on various surfaces (Abdulmajeed et al., 2011; Cho, et al., 1996; Lampin et al., 1997; Oshida et al., 1994).

In order to get these findings closer to clinical situations, in study IV, coated and non-coated zirconia were implanted in porcine gingival tissue *in vitro*. The attachment of the tissue on the implants was observed under a light microscope and immunohistochemistry was performed to detect laminin-γ-2; an

important marker in cell attachment. Laminin-γ-2 was positively stained at the junction of epithelial cells on the surface of coated implants, revealing the formation of a true attachment. This observation was absent in the case of non-coated zirconia and was coupled with frequent detachment of the tissue from its surface. In addition, the dynamic modulus of elasticity and creep modulus of the attachment between the gingiva and the implants was also evaluated under loads that mimic the mastication when implants are in function. The coated specimens demonstrated a stronger attachment and a higher creep modulus, meaning they can resist trauma and bacterial attack for longer time clinically in the oral environment.

6.2. Compressive strength (I)

The clinical behavior, limitations and potentials of dental ceramics can be predicted by assessing their strength (Guazzato et al., 2002). This can be provided by the means of flexural strength testing, since brittle ceramics are stronger in compression than tension (Della Bona et al., 2003; Duckworth, 1951).

The sol-gel coating process utilized involves re-sintering of the zirconia to stabilize the coatings on the surfaces and these temperature peaks could be a factor that can affect the strength of zirconia materials negatively. Therefore, if the coated samples are to improve the soft-tissue attachment, the coating process must have minimal effects on the physical and mechanical properties of zirconia. As a result, the biaxial flexural strengths of coated and non-coated zirconia were analyzed in study I. The coating type or method did not affect the biaxial flexural strengths and all the measurements were within the range of the values reported by other studies (Denry & Kelly, 2008; Guazzato et al., 2005; Pittayachawan et al., 2009). Temperature peaks that induce a reverse m→t transformation, hence weakening the zirconia, are in the range of 900-1000 °C. The sol-gel coating process includes heat treatments that are well below (500 °C) the range known to cause this reverse m→t transformation and therefore may not have an impact on the flexural strengths per se. However, the differences in the flexural strength values, although not significant, may be attributed to the events that occur on the surface of the coated and non-coated specimens. In study I, the biaxial flexural strength measurements were also statistically analyzed with the Weibull distribution. The Weibull modulus describes the reliability of strength or the asymmetrical strength distribution as a result of flaws and microcracks within the structure of a material (Ritter, 1995). A high Weibull modulus corresponds to fewer flaws and therefore greater structural reliability while a low Weibull modulus indicates greater flaws and defects within the material and hence a decreased reliability (Ritter, 1995). The Weibull modulus for ceramics is reported to be in the range of 5-15. Although all the specimens were found to have Weibull moduli within the reported range, the values of the coated groups and the control group were different. This difference indicates the presence of more flaws in the structure of the coated specimens and less reliability on their strength values, which may be attributed to the steps involved in the coating process. The logarithmic probability plot of the Weibull distribution also supports the inference from the calculated Weibull moduli and indicates that the non-coated control group has a higher reliability compared to the coated groups. For instance, at 5% probability of failure, a higher force is required to fracture non-coated specimens compared to coated ones. However, these differences are not significant, and the strength values are far beyond the requirements for clinical functionality (Guess et al., 2012). Just like the necessity to assess all available zirconia material for long-term clinical function, further tests are required to look at low thermal degradation behavior and fatigue testing of TiO_2 coated zirconia.

6.3. Surface characteristics (I, III)

Surface characteristics play a major role in the behavior and interaction of cells with materials. Parameters like surface hydrophilicity, roughness, surface charge, surface free energy (SFE), and morphology can influence cell adhesion, morphological change and proliferation (Abdulmajeed et al., 2011; Cho et al., 1996; Lampin et al., 1997; Oshida et al., 1994). In addition, smooth surfaces have been previously shown to facilitate epithelial cell adhesion on titanium substrates (Hormia et al., 1991).

Surfaces of the specimens were characterized using AFM and SEM examination in study I. The smoothening effect of the coatings was visible in microstructural images from AFM analysis. TiO_2 coated specimens were found to have a smoother surface when compared to the ones with ZrO_2 coating. SEM images detected presence of microcracks on the coated surfaces, which could be as a result of flaws and methodological errors involved in the specimen preparation and the coating process rather than weakness of the adhesion strength of the coatings. This is supported by the study conducted by Pätsi et al. (1998) were it was demonstrated that the adhesion strength between sol-gel derived titania coatings and the underlying titanium specimens is sufficient (>24 MPa) for their use as implant coatings. Furthermore, the cracks were only observed on polishing grooves created on the surface of the zirconia. Moreover, the presence of cracks are previously known to have no effect on cell or tissue response (Areva et al., 2004; Meretoja et al., 2010).

Study III looked at the surface wettability of the specimens by measuring the contact angles and surface free energies as predictive indices for cytocompatibility (Kasemo, 1983; Mekayarajjananonth & Winkler, 1999). Hydrophilic surfaces with higher wettability promote cell proliferation, attachment and spreading. Contact angles are measured when a drop of a liquid deposited on the surface of a solid does not spread. Theoretically, the contact angle is the angle of intersection of a line tangent to the liquid drop and the surface of the solid that it contacts. In summary, a low contact angle indicates good wettability, whereas a high contact angle indicates poor wettability (Abdulmajeed et al., 2011). Some surface wettability experiments have been previously conducted on both surface-treated and plain zirconia and titanium substrates but zirconia that is coated with TiO_2 might have differential properties (Feng et al., 2003; Watanabe et al., 2012). This is because both titania and zirconia have semiconductor and photocatalytic properties, and as a result, zirconia coated with titania might behave differently (Watanabe et al., 2012). Patel et. al. (2017) tested the potentials of zirconia coated with titanium oxide nanotube and concluded that the titania nanotubes had higher surface wettability and promoted proliferation of osteoblast cells. However, sol-gel derived titania and titania nanotubes have different surface characteristics. Study III also looked at epithelial cell attachment and proliferation onto zirconia surfaces and the SFE and contact angle measurements helped to prove the results. The contact angles were measured by taking means of 100 contact angles measured over 10 seconds on the left and right sides of 2D images of 8 droplets of each probe liquids (purely nonpolar-Formamide, polar-Diiodomethane, and hydrogen bonded-Water) settled on the sample surfaces. Furthermore, surface free energies were calculated based on contact angle data obtained using Owens-Wendt and Van-Oss methods. Both methods showed a higher total SFE for the coated specimens. The polar components of the calculated SFE of the coated zirconia using the OW method was higher, whereas the dispersive SFE of both test groups were fairly the same. This is important to notice because the behavior of cells is greatly influenced by the polar component of the SFE, which agrees with our findings. As a matter of fact, a very low polar component can inhibit cell attachment (Redey et al., 1999, 2000). Furthermore, water contact angles in the range of 50° to 65° indicate good cell adhesion and proliferation (Andrade, 1973) and water contact angles of the coated specimens lied in this range (53.0±4.8). Another component of the surface free energy to look at in this study is the fractional polarity (FP) $[\gamma^P/(\gamma^P + \gamma^D)]$ which is correlated with cell adhesion, spreading and growth

(Ponsonnet et al., 2003; Schakenraad et al., 1986). A FP of 0.3 is reported to be optimal for fibroblast compatibility and the FP of the coated specimens is in agreement with this (FP=0.3 for coated, FP=0.1 for non-coated). These properties together support the hypothesis that TiO_2 coatings can improve reaction of zirconia with soft tissue.

6.4. Blood response (II)

The formation of a healthy soft-tissue bond that will eventually block the passage of bacteria and protect the peri-implant environment, is highly dependent on the initial reactions of the abutment material with blood (Abdulmajeed et al., 2014; Davies, 2003; Park & Davies, 2000; Scheideler et al., 2007). Hemostasis, formation of a blood clot and the type of plasma proteins and blood cells adsorbed on the surface of the material are among the important factors for the healing of implants (Abdulmajeed et al., 2014; Davies, 2003; Park & Davies, 2000; Scheideler et al., 2007). The healing process starts right away when the implant is placed with adsorption of blood proteins followed by the formation of a blood clot. The formation of a blood clot is very fundamental because, it not only induces an inflammatory process that results in tissue remodeling, but it also provides a pathway for cells to migrate to the implant surface (Tord Berglundh et al., 2007; Di Iorio et al., 2005; Eming et al., 2007; Park & Davies, 2000; Salvi et al., 2015; Sculean et al., 2014; Tomasi et al., 2016). Furthermore, an important step in blood coagulation is blood platelets' activation. Platelet activation also results in release of cytokines and growth factors that are crucial for the subsequent peri-implant wound healing process (Abdulmajeed et al., 2014).

The thrombogenicity, i.e., the ability of the material to induce a blood clot, was tested in study II. In this study whole blood used was used to mimic the clinical situation where implant abutments are placed. Implant abutments contact a pool of blood at the surgical site in presence of air and this situation was mimicked by depositing fresh blood withdrawn from a healthy volunteer on the specimens. The optical densities decreased at each time-point, showing that blood coagulation was more extensive as time passed. The coated samples had more extensive blood coagulation, a phenomenon that was enhanced when the coated samples were irradiated with UV prior to the start of the experiment. UV irradiation is known to create amphiphilic and super-hydrophilic surfaces and is also used as a chairside cleansing method for implant abutments (Aita et al., 2009; Chen et al., 2015; Liu et al., 2008; Sawase et al., 2008). The most striking finding of this study was its contradicting results with the several conflicting studies on the effect of UV irradiation on blood coagulation. Some previous papers report that UV irradiation of TiO_2 surface prevents fibrinogen and platelet adhesion and therefore, conclude that anticoagulative properties are improved (Chen et al., 2015, 2014; Thevenot et al., 2008). These reports are, however based on results of experiments conducted solely with synthetic blood proteins and blood platelets while the use of fresh whole blood in study II is more justified to draw more reliable conclusions.

The adherent platelets on the surfaces after 1-hour of incubation were visualized using SEM images. Platelets on the surface of coated specimens were at a higher state of activation (early pseudopodial) compared to the other groups. The steps of platelet activation process are categorized by Goodman et al. (1984) into: (a) discoid or round; (b) dendritic; (c) early pseudopodial, spread dendritic; (d) intermediate pseudopodial, spreading and (e) fully spread. The adherent platelets on plain zirconia (dendritic) and UV treated specimens (discoid) were in a lower activated state compared to the ones on coated specimens (spread dendritic).

The adsorption of proteins on a biomaterial's surface is the first event that occurs when it comes into contact with blood (Huang et al., 2003; Milleret et al., 2015; Roy et al., 2009). For instance, albumin

adsorbed on the surface of the biomaterial will be replaced by adhesion proteins that are recognized by integrin receptors. This transforms the biomaterial, making it recognizable for subsequent adhesion of cells and consequent integration of tissue (Arima & Iwata, 2007; Díaz-Rodríguez et al., 2014). Furthermore, the extracellular matrix protein fibronectin, is known to play a role in cell attachment, spreading and differentiation in addition to platelet adhesion and aggregation (Li et al., 2011). Several studies have tested the adsorption of one or few plasma proteins on different surfaces (Cornelius et al., 2002; Dubois et al., 2009; Takami et al., 1998; Tsai et al., 2011). The design of this experiment was done to be as close as possible to a real natural clinical situation where blood proteins compete with each other on the surface of a biomaterial. The specimens were rolled in diluted human plasma in order to study the preferential adsorption of different plasma proteins on the different surfaces. Different plasma proteins (predominantly albumin) and fibronectin were adsorbed on the surfaces of all three tested groups, although no consistent differences were observed among them (Figure 13). All in all, study II showed that TiO_2 coatings promote blood coagulation, a property that is further enhanced by UV treatment. Enhanced blood coagulation results in a faster wound healing process that can be helpful in the final attachment of the abutment to the surrounding gingival tissues.

6.5. Cell response (I, III)

It has been already demonstrated that a close relationship exists between proliferating fibroblasts and the material's ability to adhere to soft tissue (Kageyama et al., 1994). Therefore, a simple fibroblast cell culture can give preliminary information about materials' biocompatibility. In study I, the specimens coated with ZrO_2 showed poor compatibility to fibroblasts. On the other hand, best results were observed with specimens coated with TiO_2, which indicate potential benefits of TiO_2 coated zirconia in soft tissue environment.

Implants lack a cementum layer and the Sharpey fibers that insert into a tooth's cementum are absent from implant surface. Most fibers in the connective tissue around implants run parallelly to its surface. This, together with other factors previously described in section 2.1., result in a compromised defense mechanism in the soft-tissue cuff around implants. Therefore, the barrier against invasion of oral bacteria primarily relies on the quality of attachment of the peri-implant epithelium and epithelial cells to the implant surface. Consequently, the behavior of epithelial cells on zirconia and on zirconia coated with TiO_2 coatings was evaluated in study III. A significant difference was observed between the 6 hour and the 24 hour with coated specimens having significantly more adherent cells. Similar observations were made during the proliferation phase of the epithelial cells. Number of cells increased on the surfaces of both test groups between each time-point (1, 3, 7 days). At each time-point, coated specimens showed a higher proliferation of epithelial cells.

According to study III, the nanoporous TiO_2 coating was able to improve the epithelial cell attachment and growth on the zirconia surface in vitro. The coatings also demonstrated a higher surface free energy and better wettability, all of which can improve the prognosis of an implant treatment through a better and firm epithelial attachment. The results support the given hypothesis, that the TiO_2 coating has the potential to promote epithelial cell attachment. This may improve the treatment results also clinically. It is noteworthy that in the presented research, the biological properties of the specimens were investigated under in vitro conditions. Soft tissue attachment on surfaces involves complex biological processes that cannot be fully imitated in laboratory conditions. Many other factors including the saliva, the immune system and other cell types can have effects on cell adhesion. Therefore, definitive conclusions can only

be drawn by further studies in real tissue environments, which was attempted in study IV, or even more accurately, in actual oral environments.

6.6. Tissue response (IV)

This study took a closer look at the morphology of tissue in contact with the materials and tested the strength of its attachment. Coated and non-coated zirconia was implanted into full-thickness porcine gingival tissue. Wong et al. 2009 demonstrated that porcine and human oral mucosal wounds are similar in terms of molecular composition and clinical and histological characteristics (Wong et al., 2009). Furthermore, in order to resemble the wound and mucoperiosteal flap created during one-stage or two-stage implant surgery in human oral mucosa, the explants were pierced with a needle prior to the placement of the sample implants. Since it was discussed in the previous section that separation of the oral cavity from the peri-implant area highly depends on the attachment of epithelium and epithelial cells onto the surface of an implant, the presence of laminin-γ-2 at the junction of epithelium and implants was regarded as a criterion for attachment in this study. This was based on the previous works of Atsuta et. al. (Atsuta et al., 2005a, 2005b) who have previously identified the presence of laminin-γ-2 in peri-implant epithelium in contact with titanium. Laminin-γ-2 was found to induce cell migration during peri-implant epithelium formation and contribute to its attachment to titanium substrates. In general, reports on soft-tissue contact with zirconia are astonishingly limited and although some reports state the presence of no difference between the tissue in contact with zirconia and titanium, others report a better biocompatibility of zirconia. The results of study IV and the distribution of laminin-γ-2 in the peri-implant epithelium around zirconia coated with TiO_2 were in agreement with the works of Atsuta et. al. The staining of laminin γ-2 –chain specific for laminin-332 in the attachment of epithelium to coated zirconia was clearly stronger than in the attachment of epithelium to uncoated zirconia. Although sloughing of epithelial cells was identified within the surface of the tissue explants, the bond of the epithelium to the coated implants seemed to be unaffected. The results of the dynamic modulus analyses performed also support these histological findings. It may be inferred that tissue attachment to zirconia abutments is inferior to that of titanium and that zirconia abutments require further optimization to achieve soft-tissue attachment. This optimization was attempted in this thesis through sol-gel derived TiO_2 coatings.

Most soft connective tissues, including the gingival tissue, and the attachment apparatus formed between them and a dental implant abutment are viscoelastic in nature (Burton et al., 2017; Craiem & Armentano, 2007; Gow & Taylor, 1968; Holzapfel et al., 2002). A viscoelastic material is a material that exhibits both elastic and viscous characteristics, i.e., its behavior contains both elastic and dissipative components of deformation (Peterson et al., 2015; Saber-Sheikh et al., 1999). Elastic materials deform under stress and return to their original state when the stress is removed, while viscous materials return over time to a state similar, but not identical, to the original state (Peterson et al., 2015). In addition, teeth, gingival tissue and dental materials including implants, are constantly subject to repetitive forces of mastication. For such materials, dynamic tests such as dynamic mechanical analysis provide more relevant information about their properties than traditional static tests. Study IV involved the application of oscillating forces in shear, similar to that of mastication at the physiological frequency (1 Hz), to the specimens and the response of the attachment apparatus to deformation was analyzed. For assessment of realistic stresses and displacements a 2D-axyisymmetric model was set up (COMSOL Multiphysics 5.3, Comsol Inc.) to estimate the distribution of the deformation inside the soft tissue attached to the abutment assuming the latter to be a rigid solid. This model was served as a visual guidance as exact properties of the soft tissue are not known in these conditions. Figure 20 shows maximal total displacements (color

scale), surface traction forces (vector arrows) and von Mises stresses (contours), which indicate that most of the traction forces are indeed localized at the tissue/abutment interface. The higher dynamic modulus reported with zirconia coated with TiO_2 specimens, together with the immunohistochemical analyses, translate to a stronger attachment with the surrounding tissue. Similarly, under creeping conditions, a higher force will be required to creep zirconia coated with TiO_2 to the same arbitrary deformation when compared to non-coated implant/tissue complexes. The clinical implication of this study is that the coated abutments will have a stronger attachment to the surrounding gingiva and hence resist trauma and bacterial attack for a longer time. The coatings help in providing a separation of the intraoral and peri-implant environments, and their attachment to the surrounding soft tissue undergoes less deformation over time when the implants are in function.

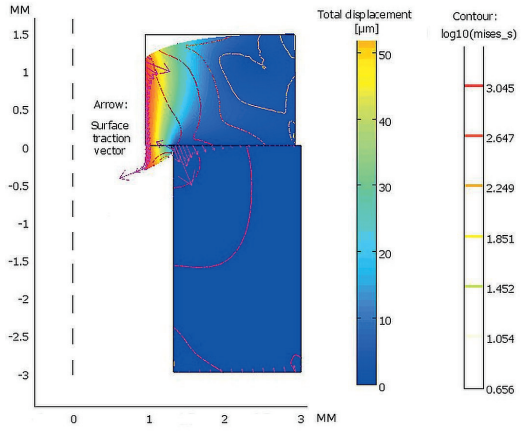

Figure 20 *Computer model showing symmetric part of the tissue and the support with displacements, stresses and traction forces.*

6.7. Future prospective

There is a lack of research and understanding about soft-tissue interface with implant abutment materials. Further general research related to this topic is necessary. In this thesis, the biological response to zirconia and zirconia coated with nanoporous TiO_2 coatings was explored under in vitro conditions. Non-coated zirconia was proved to be inferior compared to the coated ones and this indicates the necessity of research aimed at optimizing commercially available zirconia abutments for soft-tissue integration.

Long term clinical follow-up of zirconia abutments is still needed to draw conclusive decisions about the functionality of this material as an implant abutment. Nevertheless, more research is also needed to understand the superior properties of the coated specimens indicated in this thesis. *In vivo* test conditions and long-term clinical trials and follow-ups in human subjects will facilitate a more direct correlation and support of these findings.

7. CONCLUSIONS

Based on the studies and the results of the experiments reported in this thesis, the following can be concluded:

1. The biaxial flexural strength of zirconia is unaffected by sol-gel derived coatings of TiO_2.

2. TiO_2 coatings promote blood coagulation, a property that is further enhanced by UV treatment. Furthermore, TiO_2 coatings alone also promoted platelet adhesion and activation.

3. Sol-gel-derived TiO_2 -coating is able to improve the adhesion and proliferation of human gingival epithelial cells on zirconia in vitro.

4. Coated surfaces have better wettability and higher SFE, meaning they have a potential to better assist the formation of an epithelial junction to the surface of an implant abutment.

5. Sol-gel derived TiO_2 coatings on zirconia were proven to enhance soft tissue attachment, forming a stronger adhesion between the gingival tissue in contact with TiO_2 coatings under physiological dynamic loading.

Different tissue structures and components in the oral cavity were proven to favor zirconia coated with sol-gel derived TiO_2. Therefore, it can be concluded that nonporous TiO_2 coatings have good potential to enhance gingival tissue integration on zirconia dental implant abutments.

ACKNOWLEDGEMENTS

Praises and thanks be to God, who is the Lord of the universe, for easing the path, by blessing me with determination, health, and surrounding me with supportive and loving people, to accomplish my goals.

I offer my sincerest and profound gratitude to my supervisor Prof. Timo Närhi for accepting me as a PhD student and for all his exceptional support during my journey. He guided me throughout every process and assigned me with different duties and responsibilities that allowed me to grow as a research scientist. He offered his exceptional support in all the ups and downs of the journey. One could simply not wish for a better supervisor.

I was very fortunate to have Dr. Aous Abdulmajeed as my second supervisor. Dr. Aous is more than just an academic supervisor to me. He is an elder brother who took me by the hand and taught me how to take baby-steps of research and contributing to science. Dr. Aous is the reason I am in Finland; the person who introduced me to the PhD program at the University of Turku and to Prof. Timo Närhi. I am forever grateful.

I am grateful to Prof. Pekka Vallittu, the dean of Institute of Dentistry, University of Turku for creating a unique, supportive environment by providing all the means necessary to allow researchers perform their best. Your contribution to the field of biomaterials is inspiring and you are a role model to all young scientists.

My work station is at the Turku Clinical Biomaterials Center (TCBC). The PhD journey would have been impossible without Dr. Lippo Lassila, the head of TCBC and our Great Sauna Master. The Sauna Project™ has been always a priority and an integral part of the PhD journey. Thank you for creating the most fun work environment anyone could ask for, for introducing me to the authentic Finnish lifestyle, and for giving me great tips in both research and life.

I thank Finnish Doctoral Program in Oral Sciences (FINDOS) for providing me the financial support to be able to focus better on the research work.

I am thankful to all the co-authors who contributed to my scientific articles; Dr. Heidi Leminen, Dr. Ville Meretoja, Paula Linderbäck, Dr. Sini Riivari, and Frank Wallboomers. Special thanks to the great Prof. Eva Söderling, Dr. Jaana Willberg, and Dr. Michael Gasik, who granted me their valuable time at many occasions and taught me essential scientific lessons.

Thanks to ID Creations Oy, Antti Kangasniemi and especially Dr. Ilkka Kangasniemi, for all their constant help throughout the project.

Special warm thanks to the always welcoming, helpful, happy, and kind masters; Katja Sampalahti, Oona Hällfors, Mariia Valkama for their excellent and skilled technical assistance during the lab-works of the studies involved in this thesis.

I appreciate having awesome coworkers around me at TCBC; Dr. Yulia Kolkova and her life-saving tips, Dr. Niko Moritz - a great scientist who I look forward to work with, мой лучший русский друг - Artem Plyusnin and his lovely family, Dr. Shinji Yoshii, Dr. Sofyan Garoushi, Dr. Jasmina Bijelic, Dr. Leila

Perea-Lowery, Dr. Mervi Puska and Dr. Mona Gibreel for their kind support. I am thankful to Päivi Haaranen, Anna Kostiander, and especially Genevieve Alfont for their assistance and guidance in the labs at TCBC.

I would like to mention Dr. Michael Nelson and thank him substantially for advancing my English academic writing and presentation skills. For trusting me and providing me the opportunity to give workshops hand-in-hand with my brother, Dr. Tarek Omran, to other PhD candidates at the University of Turku.

I thank Anni Itähaarla, perhaps the best Finnish teacher in the World, for all her efforts in teaching me the Finnish language. Kiitos paras opettaja maailmassa.

During the first few months of my stay in Turku, I worked closely with Dr. Taiseer Sulaiman and had the pleasure to coauthor two articles with him. Thank you very much for giving me the opportunity to be on your side and to learn from you. You are a great, knowledgeable scientist and a super fun elder brother. Meeting you, your brothers Dr. Aous and Dr. Awab, is one of the best highlights of my life. Thank you all, and God bless you and your mother, and father Prof. Abdulhaq, for upbringing you lovely people.

Finland right away became Funland by meeting people who paved the road to the completion of this wonderful journey. Words cannot express how grateful I am to Hameed Hussain (Hameed Chacha), Ghasim Al Rammahi (Abu Mohammad), Dr. Jongyun Moon and Dr. Wael Rihan for their guidance and support. You made Finland feel like home in many ways possible. I spent only a few months with Dr. Masahiko Kobayashi upon my arrival in Finland, however, we built a forever lasting friendship and brotherhood that simply cannot be explained. I admire you Kobayashi Sensei and it is an honor to have known you. Siawashena Tanjobino Kobayashi Sensei. Kiitos Sauna Pekka, you make every sauna experience fun and exceptional.

My valuable circle of friends has been a source of positive energy and a driving force in my life. Friends that are not friends, but family who have been on my side for at least the past 10 year despite the fact that we are scattered all around the World; Dr. Faraj Edher, Dr. Modar Qais, Dr. Karim Salah, Dr. Shehreyar Chaudhry, Dr. Sara Anbari and Dr. Lina Eid. My very supportive and most fun brothers that simply make every second of my life more cheerful and happier; Omar Salah (Omar TNT), Ahmad Salah, Ibrahim Qasim (breaky), Abdulrahman Nawar (Abdo), Ahmed Elmahdi (El-Mandi), Saman Hosseini and Ehsan Pishdast (Pishi). My loved ones in Turku; my amazing, successful brothers that taekwondo brought us together - Sanan Eskandari, Ahmed Abdulghani and Elom Damalie. The aito päälliköt that I will miss if I don't meet them for one day; Rizgar Yusif, Oliver Liesmäki and Sami Köseoglu. The person who I spent some of the most memorable times with and I love from the bottom of my heart, Kaveri Dr. Henri Ailio and his family. My super fun Bestis, a source of constant good vibes; Ella Suppala and her family. The pure hearted Asta Soiniitty who made Finnish summers a unique experience for us at her cottage. The great role model and a person to learn from; Markus Hyry and his lovely family. My very, very intellectual and knowledgeable brother; Oliver Briny. Finland's best-selling author and a good friend; Juhana Torkki. My first ever and oldest Finnish friends who helped me settle in Finland; Dr. Annina Salmi and Dr. Heidi Ekholm. Dr. Liisa Lehto for being so kind all the time in every way possible. Great souls that I will forever have in my heart; Dr. Morta Stasikėlytė, Noora Wilén, Henna Ilona Laakso, Dr. Aaro Turunen, Dr. Jeremias, Edona Jetullahi, Savior Husaini, Muha Altug, Zafer Kaymaz, Petra Parviainen, Petrus Kurppa, Kaveh Nikjamal, Obada Alzghool, Jamal (Jaymz), Ali Benkherouf, Ismail

Mohammadi, Dr. Nagat Areid, Dr. Faleh Abushahba, Dr. Ahmed El-Gahawy, Richard and Robin Rajala, Ardijan Ibrahimi, Jens Tuovinen and many others.

This thesis is dedicated to my family and mentors. Meeting Dr. Aous and hence coming to Finland would not have been possible without Dr. Ahmed Osman, a great teacher of dentistry and a mentor. Thank you, Dr. Ahmed, for noticing my interest in dental materials and research, and for facilitating this phase of my career as a dentist.

I would like to also sincerely thank Prof. Richard Simonsen. You enlightened your students with your great experience and knowledge and taught us ethics in both life and dentistry. Your quote of "the harder you work, the luckier you get" resonates in our head. Thank you for your kind support during the years and all the great lessons you have taught us.

Lastly, and most importantly, my family. What can I say about the people behind everything good that has happened to me in my life? My dearest two people in the World, mom and dad, your love, your teachings, your sacrifices, your support and the hardships you took so your children will have a good life is what has made this journey possible. My one and only, beautiful sister Dr. Zahra Shahramian who's love and caring is beyond what any brother would dream for. My second family, the Omran family, the lovely Captain Ashraf Omran and Dr. Samia Khedr who blessed this World with two pure souls, Hesham Omran and most importantly, my backbone, my support, my companion, the person who helped me get up every time I fell down, my bright, true brother; Dr. Tarek Omran. Words cannot express my love to you all.

Turku 20.03.2019

Khalil Shahramian

REFERENCES

A. Sulaiman, T., A. Abdulmajeed, A., E. Donovan, T., K. Vallittu, P., O. Närhi, T., & V. Lassila, L. (2015). The effect of staining and vacuum sintering on optical and mechanical properties of partially and fully stabilized monolithic zirconia. *Dental Materials Journal*, *34*(5), 605–610.

Ääritalo, V., Areva, S., Jokinen, M., Lindén, M., & Peltola, T. (2007). Sol-gel-derived TiO2–SiO2 implant coatings for direct tissue attachment. Part I: design, preparation and characterization. *Journal of Materials Science: Materials in Medicine*, *18*(9), 1863–1873.

Abdulmajeed, A. A., Lassila, L. V, Vallittu, P. K., & Närhi, T. O. (2011). The effect of exposed glass fibers and particles of bioactive glass on the surface wettability of composite implants. *International Journal of Biomaterials*, *2011*, 607971.

Abdulmajeed, A. A., Walboomers, X. F., Massera, J., Kokkari, A. K., Vallittu, P. K., & Närhi, T. O. (2014). Blood and fibroblast responses to thermoset BisGMA-TEGDMA/glass fiber-reinforced composite implants *in vitro*. *Clinical Oral Implants Research*, *25*(7), 843–851.

Abdulmajeed, A. A., Willberg, J., Syrjänen, S., Vallittu, P. K., & Närhi, T. O. (2015). In vitro assessment of the soft tissue/implant interface using porcine gingival explants. *Journal of Materials Science: Materials in Medicine*, *26*(1), 1–7.

Abrahamsson, lngemar, Berglundh, T., & Lindhe, J. (1998). Soft tissue response to plaque formation at different implant systems. A comparative study in the dog. *Clinical Oral Implants Research*, *9*(2), 73–79.

Abrahamsson, I., Zitzmann, N. U., Berglundh, T., Linder, E., Wennerberg, A., & Lindhe, J. (2002). The mucosal attachment to titanium implants with different surface characteristics: An experimental study in dogs. *Journal of Clinical Periodontology*, *29*(5), 448–455.

Advincula, M. C., Rahemtulla, F. G., Advincula, R. C., Ada, E. T., Lemons, J. E., & Bellis, S. L. (2006). Osteoblast adhesion and matrix mineralization on sol–gel-derived titanium oxide. *Biomaterials*, *27*(10), 2201–2212.

Aita, H., Hori, N., Takeuchi, M., Suzuki, T., Yamada, M., Anpo, M., & Ogawa, T. (2009). The effect of ultraviolet functionalization of titanium on integration with bone. *Biomaterials*, *30*(6), 1015–1025.

Al-Ahmad, A., Wiedmann-Al-Ahmad, M., Faust, J., Bächle, M., Follo, M., Wolkewitz, M., … Kohal, R. (2010). Biofilm formation and composition on different implant materials in vivo. *Journal of Biomedical Materials Research Part B: Applied Biomaterials*, *95B*(1), 101–109.

Al-Nawas, B., Groetz, K. A., Goetz, H., Duschner, H., & Wagner, W. (2008). Comparative histomorphometry and resonance frequency analysis of implants with moderately rough surfaces in a loaded animal model. *Clinical Oral Implants Research*, *19*, 1–8.

Albrektsson, T., & Isidor, F. (1994). Consensus report of session IV. In N. P. Lang & T. Karring (Eds.), *Proceeding of the 1st European workshop on periodontology* (pp. 365–369). Quintessence Publishing Co.

Altankov, G., Grinnell, F., & Groth, T. (1996). Studies on the biocompatibility of materials: Fibroblast reorganization of substratum-bound fibronectin on surfaces varying in wettability. *Journal of Biomedical Materials Research*, *30*(3), 385–391.

Andersson, B., Glauser, R., Maglione, M., & Taylor, A. (2003). Ceramic implant abutments for short-span FPDs: a prospective 5-year multicenter study. *The International Journal of Prosthodontics*, *16*(6), 640–646.

Andersson, B., Taylor, A., Lang, B. R., Scheller, H., Schärer, P., Sorensen, J. A., & Tarnow, D. (2001). Alumina ceramic implant abutments used for single-tooth replacement: a prospective 1- to 3-year multicenter study. *The International Journal of Prosthodontics*, *14*(5), 432–438.

Andrade, J. D. (1973). Interfacial phenomena and biomaterials. *Medical Instrumentation*, *7*(2), 110–119.

Andreiotelli, M., Wenz, H. J., & Kohal, R.-J. (2009). Are ceramic implants a viable alternative to titanium implants? A systematic literature review. *Clinical Oral Implants Research*, *20*, 32–47.

Andrukhov, O., Huber, R., Shi, B., Berner, S., Rausch-Fan, X., Moritz, A., … Schedle, A. (2016). Proliferation, behavior, and differentiation of osteoblasts on surfaces of different microroughness. *Dental Materials*, *32*(11), 1374–1384.

Araujo, M. G., & Lindhe, J. (2018). Peri-implant health. *Journal of Clinical Periodontology*, *45*, S230–S236.

Areva, S., Ääritalo, V., Tuusa, S., Jokinen, M., Lindén, M., & Peltola, T. (2007). Sol-Gel-derived TiO2–SiO2 implant coatings for direct tissue attachment. Part II: Evaluation of cell response. *Journal of Materials Science: Materials in Medicine*, *18*(8), 1633–1642.

Areva, S., Paldan, H., Peltola, T., Närhi, T., Jokinen, M., & Lindén, M. (2004). Use of sol-gel-derived titania coating for direct soft tissue attachment. *Journal of Biomedical Materials Research Part A*, *70A*(2), 169–178.

Arima, Y., & Iwata, H. (2007). Effect of wettability and surface functional groups on protein adsorption and cell adhesion using well-defined mixed self-assembled monolayers. *Biomaterials*, *28*(20), 3074–3082.

Atsuta, I., Yamaza, T., Yoshinari, M., Goto, T., Kido, M. A., Kagiya, T., … Tanaka, T. (2005). Ultrastructural localization of laminin-5 (γ2 chain) in the rat peri-implant oral mucosa around a titanium-dental implant by immuno-electron microscopy. *Biomaterials*, *26*(32), 6280–6287.

Atsuta, I., Yamaza, T., Yoshinari, M., Mino, S., Goto, T., Kido, M. A., … Tanaka, T. (2005). Changes in the distribution of laminin-5 during peri-implant epithelium formation after immediate titanium implantation in rats. *Biomaterials*, *26*(14), 1751–1760.

Baier, R. E., Meyer, A. E., Natiella, J. R., Natiella, R. R., & Carter, J. M. (1984). Surface properties determine bioadhesive outcomes: Methods and results. *Journal of Biomedical Materials Research*, *18*(4), 337–355.

Bako, P., Bassiouni, M., Eckhard, A., Gerlinger, I., Frick, C., Löwenheim, H., & Müller, M. (2015). Methyl methacrylate embedding to study the morphology and immunohistochemistry of adult guinea pig and mouse cochleae. *Journal of Neuroscience Methods*, *254*, 86–93.

Berglundh, T., Abrahamsson, I., Welander, M., Lang, N. P., & Lindhe, J. (2007). Morphogenesis of the peri-implant mucosa: an experimental study in dogs. *Clinical Oral Implants Research*, *18*(1), 1–8.

Berglundh, T., Lindhe, J., Ericsson, I., Marinello, C. P., Liljenberg, B., & Thornsen, P. (1991). The soft tissue barrier at implants and teeth. *Clinical Oral Implants Research*, *2*(2), 81–90.

Block, M. S., Kent, J. N., & Kay, J. F. (1987). Evaluation of hydroxylapatite-coated titanium dental implants in dogs. *Journal of Oral and Maxillofacial Surgery*, *45*(7), 601–607.

Bosshardt, D. D., & Lang, N. P. (2005). The junctional epithelium: From health to disease. *Journal of Dental Research*, *84*(1), 9–20.

Bürgers, R., Gerlach, T., Hahnel, S., Schwarz, F., Handel, G., & Gosau, M. (2010). In vivo and in vitro biofilm formation on two different titanium implant surfaces. *Clinical Oral Implants Research*, *21*(2), 156–164.

Burton, H. E., Freij, J. M., & Espino, D. M. (2017). Dynamic Viscoelasticity and Surface Properties of Porcine Left Anterior Descending Coronary Arteries. *Cardiovascular Engineering and Technology*, *8*(1), 41–56.

Buser, D., Weber, H. P., Donath, K., Fiorellini, J. P., Paquette, D. W., & Williams, R. C. (1992). Soft Tissue Reactions to Non-Submerged Unloaded Titanium Implants in Beagle Dogs. *Journal of Periodontology*, *63*(3), 225–235.

Carcuac, O., Abrahamsson, I., Albouy, J.-P., Linder, E., Larsson, L., & Berglundh, T. (2013). Experimental periodontitis and peri-implantitis in dogs. *Clinical Oral Implants Research*, *24*(4), 363–371.

Carcuac, O., & Berglundh, T. (2014). Composition of Human Peri-implantitis and Periodontitis Lesions. *Journal of Dental Research*, *93*(11), 1083–1088.

Cate, T., & Nanci, A. (2017). *Ten Cate's oral histology : development, structure, and function*. (Antonio Nanci, Ed.) (9th ed.). St Louis, Missouri: Elsevier Mosby.

Chai, W. L., Moharamzadeh, K., Brook, I. M., Emanuelsson, L., Palmquist, A., & van Noort, R. (2010). Development of a Novel Model for the Investigation of Implant–Soft Tissue Interface. *Journal of Periodontology*, *81*(8), 1187–1195.

Chen, J., Yang, P., Liao, Y., Wang, J., Chen, H., Sun, H., & Huang, N. (2015). Effect of the Duration of UV Irradiation on the Anticoagulant Properties of Titanium Dioxide Films. *ASC Applied Materials & Interfaces*, *7*, 4423–4432.

Chen, J., Zhao, A., Chen, H., Liao, Y., Yang, P., Sun, H., & Huang, N. (2014). The effect of full/partial UV-irradiation of TiO2 films on altering the behavior of fibrinogen and platelets. *Colloids and Surfaces B: Biointerfaces*, *122*, 709–718.

Cho, C.-S., Kobayashi, A., Goto, M., Akaike, T., & Park, K.-H. (1996). Difference in adhesion and proliferation of fibroblast between Langmuir-Blodgett films and cast surfaces of poly(?-benzyl L-glutamate)/poly(ethylene oxide) diblock copolymer. *Journal of Biomedical Materials Research*, *32*(3), 425–432.

Clark, R. A. F., Lin, F., Greiling, D., An, J., & Couchman, J. R. (2004). Fibroblast Invasive Migration into Fibronectin/Fibrin Gels Requires a Previously Uncharacterized Dermatan Sulfate-CD44 Proteoglycan. *Journal of Investigative Dermatology*, *122*(2), 266–277.

Coelho, P. G., Granjeiro, J. M., Romanos, G. E., Suzuki, M., Silva, N. R. F., Cardaropoli, G., … Lemons, J. E. (2009). Basic research methods and current trends of dental implant surfaces. *Journal of Biomedical Materials Research Part B: Applied Biomaterials*, *88B*(2), 579–596.

Coray, R., Zeltner, M., & Özcan, M. (2016). Fracture strength of implant abutments after fatigue testing: A systematic review and a meta-analysis. *Journal of the Mechanical Behavior of Biomedical Materials*, *62*, 333–346.

Cornelius, R. M., Archambault, J., & Brash, J. L. (2002). Identification of apolipoprotein A-I as a major adsorbate on biomaterial surfaces after blood or plasma contact. *Biomaterials*, *23*(17), 3583–3587.

Costa, F. O., Takenaka-Martinez, S., Cota, L. O. M., Ferreira, S. D., Silva, G. L. M., & Costa, J. E. (2012). Peri-implant disease in subjects with and without preventive maintenance: a 5-year follow-up. *Journal of Clinical Periodontology*, *39*(2), 173–181.

Craiem, D., & Armentano, R. L. (2007). A fractional derivative model to describe arterial viscoelasticitye. *Biorheology*, *44*(4), 251–263.

Davies, J. (2003). Understanding peri-implant endosseous healing. *Journal of Dental Education*, *67*(8), 932–949.

Degidi, M., Artese, L., Scarano, A., Perrotti, V., Gehrke, P., & Piattelli, A. (2006). Inflammatory Infiltrate, Microvessel Density, Nitric Oxide Synthase Expression, Vascular Endothelial Growth Factor Expression, and Proliferative Activity in Peri-Implant Soft Tissues Around Titanium and Zirconium Oxide Healing Caps. *Journal of Periodontology*, *77*(1), 73–80.

Della Bona, A., Anusavice, K. J., & DeHoff, P. H. (2003). Weibull analysis and flexural strength of hot-pressed core and veneered ceramic structures. *Dental Materials*, *19*(7), 662–669.

Denry, I., & Kelly, J. R. (2008). State of the art of zirconia for dental applications. *Dental Materials*, *24*(3), 299–307.

DePalma, V. A., Baier, R. E., Ford, J. W., Gott, V. L., & Furuse, A. (1972). Investigation of three-surface properties of several metals and their relation to blood compatibility. *Journal of Biomedical Materials Research*, *6*(4), 37–75.

Derks, J., & Tomasi, C. (2015). Peri-implant health and disease. A systematic review of current epidemiology. *Journal of Clinical Periodontology*, *42*, S158–S171.

Di Iorio, D., Traini, T., Degidi, M., Caputi, S., Neugebauer, J., & Piattelli, A. (2005). Quantitative Evaluation of the Fibrin Clot Extension on Different Implant Surfaces: An In Vitro Study. *Journal of Biomedical Materials Research - Part B Applied Biomaterials*, *74B*(1), 636–642.

Díaz-Rodríguez, P., González, P., Serra, J., & Landin, M. (2014). Key parameters in blood-surface interactions of 3D bioinspired ceramic materials. *Materials Science and Engineering: C*, *41*, 232–239.

Dickinson, D. P., Coleman, B. G., Batrice, N., Lee, J., Koli, K., Pennington, C., … Wikesjö, U. M. E. (2013). Events of wound healing/regeneration in the canine supraalveolar periodontal defect model. *Journal of Clinical Periodontology*, *40*(5), 527–541.

Doundoulakis, J. H. (1987). Surface analysis of titanium after sterilization: Role in implant-tissue interface and bioadhesion. *The Journal of Prosthetic Dentistry*, *58*(4), 471–478.

Dubois, J., Gaudreault, C., & Vermette, P. (2009). Biofouling of dextran-derivative layers investigated by quartz crystal microbalance. *Colloids and Surfaces B: Biointerfaces*, *71*(2), 293–299.

Duckworth, W. H. (1951). Precise Tensile Properties of Ceramic Bodies. *Journal of the American Ceramic Society*, *34*(1), 1–9.

Eggers, G., Rieker, M., Kress, B., Fiebach, J., Dickhaus, H., & Hassfeld, S. (2005). Artefacts in magnetic resonance imaging caused by dental material. *Magnetic Resonance Materials in Physics, Biology and Medicine*, *18*(2), 103–111.

Emecen-Huja, P., Eubank, T. D., Shapiro, V., Yildiz, V., Tatakis, D. N., & Leblebicioglu, B. (2013). Peri-implant versus periodontal wound healing. *Journal of Clinical Periodontology*, *40*(8), 816–824.

Eming, S. A., Krieg, T., & Davidson, J. M. (2007). Inflammation in Wound Repair: Molecular and Cellular Mechanisms. *Journal of Investigative Dermatology*, *127*(3), 514–525.

Feng, B., Weng, J., Yang, B. C., Qu, S. X., & Zhang, X. D. (2003). Characterization of surface oxide films on titanium and adhesion of osteoblast.

Biomaterials, *24*(25), 4663–4670.

Fujishima, A., Rao, T. N., & Tryk, D. A. (2000). Titanium dioxide photocatalysis. *Journal of Photochemistry and Photobiology C: Photochemistry Reviews*, *1*(1), 1–21.

Gahlert, M., Burtscher, D., Grunert, I., Kniha, H., & Steinhauser, E. (2012). Failure analysis of fractured dental zirconia implants. *Clinical Oral Implants Research*, *23*(3), 287–293.

Giavaresi, G., Fini, M., Cigada, A., Chiesa, R., Rondelli, G., Rimondini, L., … Giardino, R. (2003). Histomorphometric and microhardness assessments of sheep cortical bone surrounding titanium implants with different surface treatments. *Journal of Biomedical Materials Research*, *67A*(1), 112–120.

Goodman, S. L., Lelah, M. D., Lambrecht, L. K., Cooper, S. L., & Albrecht, R. M. (1984). In vitro vs. ex vivo platelet deposition on polymer surfaces. *Scanning Electron Microscopy*, (Pt 1), 279–290.

Gotfredsen, K., Berglundh, T., & Lindhe, J. (2000). Anchorage of Titanium Implants with Different Surface Characteristics: An Experimental Study in Rabbits. *Clinical Implant Dentistry and Related Research*, *2*(3), 120–128.

Gow, B. S., & Taylor, M. G. (1968). Measurement of viscoelastic properties of the aorta in the living dog. *Circulation Research*, *23*(2), 111–122.

Grant DA, Stern IB, Listgarten MA (eds), with 18 contributors. (1987). *Periodontics, 6th ed*. St. Louis: C.V. Mosby.

Grossner-Schreiber, B., Griepentrog, M., Haustein, I., Muller, W.-D., Briedigkeit, H., Gobel, U. B., & Lange, K.-P. (2001). Plaque formation on surface modified dental implants. An in vitro study. *Clinical Oral Implants Research*, *12*(6), 543–551.

Guazzato, M., Albakry, M., Swain, M. V., & Ironside, J. (2002). Mechanical properties of In-Ceram Alumina and In-Ceram Zirconia. *The International Journal of Prosthodontics*, *15*(4), 339–346.

Guazzato, M., Quach, L., Albakry, M., & Swain, M. V. (2005). Influence of surface and heat treatments on the flexural strength of Y-TZP dental ceramic. *Journal of Dentistry*, *33*(1), 9–18.

Guess, P. C., Att, W., & Strub, J. R. (2012). Zirconia in Fixed Implant Prosthodontics. *Clinical Implant Dentistry and Related Research*, *14*(5), 633–645.

Hallab, N. J., Bundy, K. J., O'Connor, K., Clark, R., & Moses, R. L. (1995). Cell adhesion to biomaterials: correlations between surface charge, surface roughness, adsorbed protein, and cell morphology. *Journal of Long-Term Effects of Medical Implants*, *5*(3), 209–231.

Hamdan, M., Blanco, L., Khraisat, A., & Tresguerres, I. F. (2006). Influence of Titanium Surface Charge on Fibroblast Adhesion. *Clinical Implant Dentistry and Related Research*, *8*(1), 32–38.

Heffernan, M. J., Aquilino, S. A., Diaz-Arnold, A. M., Haselton, D. R., Stanford, C. M., & Vargas, M. A. (2002). Relative translucency of six all-ceramic systems. Part I: Core materials. *The Journal of Prosthetic Dentistry*, *88*(1), 4–9.

Heitz-Mayfield, L. J. A., & Salvi, G. E. (2018). Peri-implant mucositis. *Journal of Periodontology*, *89*, S257–S266.

Henriksson, K., & Jemt, T. (2003). Evaluation of custom-made procera ceramic abutments for single-implant tooth replacement: a prospective 1-year follow-up study. *The International Journal of Prosthodontics*, *16*(6), 626–630.

Hisbergues, M., Vendeville, S., & Vendeville, P. (2008). Zirconia: Established facts and perspectives for a biomaterial in dental implantology. *Journal of Biomedical Materials Research Part B: Applied Biomaterials*, *88B*(2), 519–529.

Höland, W., Schweiger, M., Watzke, R., Peschke, A., & Kappert, H. (2008). Ceramics as biomaterials for dental restoration. *Expert Review of Medical Devices*, *5*(6), 729–745.

Holzapfel, G. A., Gasser, T. C., & Stadler, M. (2002). A structural model for the viscoelastic behavior of arterial walls: Continuum formulation and finite element analysis. *European Journal of Mechanics, A/Solids*, *21*(3), 441–463.

Hormia, M., Kononen, M., Kivilahti, J., & Virtanen, I. (1991). Immunolocalization of proteins specific for adhaerens junctions in human gingival epithelial cells grown on differently processed titanium surfaces. *Journal of Periodontal Research*, *26*(6), 491–497.

Hosseini, M., Worsaae, N., Schiødt, M., & Gotfredsen, K. (2013). A 3-year prospective study of implant-supported, single-tooth restorations of all-ceramic and metal-ceramic materials in patients with tooth agenesis. *Clinical Oral Implants Research*, *24*(10), 1078–1087.

Huang, N., Yang, P., Leng, Y. X., Chen, J. Y., Sun, H., Wang, J., … Leng, Y. (2003). Hemocompatibility of titanium oxide films. *Biomaterials*, *24*(13), 2177–2187.

Ivanoff, C.-J., Sennerby, L., Johansson, C., Rangert, B., & Lekholm, U. (1997). Influence of implant diameters on the integration of screw implants: An experimental study in rabbits. *International Journal of Oral and Maxillofacial Surgery*, *26*(2), 141–148.

Ivanovski, S., & Lee, R. (2018). Comparison of peri-implant and periodontal marginal soft tissues in health and disease. *Periodontology 2000*, *76*(1), 116–130.

Jepsen, S., Berglundh, T., Genco, R., Aass, A. M., Demirel, K., Derks, J., … Zitzmann, N. U. (2015). Primary prevention of peri-implantitis: Managing peri-implant mucositis. *Journal of Clinical Periodontology*, *42*, S152–S157.

Jokinen, M., Pätsi, M., Rahiala, H., Peltola, T., Ritala, M., & Rosenholm, J. B. (1998). Influence of sol and surface properties onin vitro bioactivity of sol-gel-derived TiO2 and TiO2-SiO2 films deposited by dip-coating method. *Journal of Biomedical Materials Research*, *42*(2), 295–302.

Kageyama, Y., Yokoyama, Y., Suzuki, K., Harada, Y., & Kokubo, T. (1994). Response of Soft Tissue Against Hydroxyapatite Coated on Polymers. *Bioceramics*, 165–170.

Kajiwara, N., Masaki, C., Mukaibo, T., Kondo, Y., Nakamoto, T., & Hosokawa, R. (2015). Soft tissue biological response to zirconia and metal implant abutments compared with natural tooth: Microcirculation monitoring as a novel bioindicator. *Implant Dentistry*, *24*(1), 37–41.

Kamel, E. M., Burger, C., Buck, A., von Schulthess, G. K., & Goerres, G. W. (2003). Impact of metallic dental implants on CT-based attenuation correction in a combined PET/CT scanner. *European Radiology*, *13*(4), 724–728.

Kasemo, B. (1983). Biocompatibility of titanium implants: Surface science aspects. *The Journal of Prosthetic Dentistry*, *49*(6), 832–837.

Kasemo, B., & Lausmaa, J. (1985). Metal Selection and Surface Characteristics. In G. A. Z. and T. A. P.-I. Branemark (Ed.), *Tissue-Integrated Prostheses: Osseointegration in Clinical Dentistry* (pp. 99–116). Chicago: Quintessence Publishing Co.

Kim, Y.-S., Shin, S.-Y., Moon, S.-K., & Yang, S.-M. (2015). Surface properties correlated with the human gingival fibroblasts attachment on various materials for implant abutments: A multiple regression analysis. *Acta Odontologica Scandinavica*, *73*(1), 38–47.

Lacefield, W. R. (1988). Hydroxyapatite Coatings. *Annals of the New York Academy of Sciences*, *523*(1 Bioceramics), 72–80.

Lacefield, W. R. (1998). Current status of ceramic coatings for dental implants. *Implant Dentistry*, *7*(4), 315–322.

Lacoste-Ferré, M. H., Demont, P., Dandurand, J., Dantras, E., Duran, D., & Lacabanne, C. (2011). Dynamic mechanical properties of oral mucosa: Comparison with polymeric soft denture liners. *Journal of the Mechanical Behavior of Biomedical Materials*, *4*(3), 269–274.

Lampin, M., Warocquier-Clérout, R., Legris, C., Degrange, M., & Sigot-Luizard, M. F. (1997). Correlation between substratum roughness and wettability, cell adhesion, and cell migration. *Journal of Biomedical Materials Research*, *36*(1), 99–108.

Lang, N. P., & Berglundh, T. (2011). Periimplant diseases: where are we now? - Consensus of the Seventh European Workshop on Periodontology. *Journal of Clinical Periodontology*, *38*, 178–181.

Lemons, J. E., Misch-Dietsh, F., & McCracken, M. S. (2015). Biomaterials for Dental Implants. In *Dental Implant Prosthetics* (pp. 66–94). Elsevier.

Li, G., Yang, P., Liao, Y., & Huang, N. (2011). Tailoring of the Titanium Surface by Immobilization of Heparin/ Fibronectin Complexes for Improving Blood Compatibility and Endothelialization: An in Vitro Study. *Biomacromolecules*, *12*, 1155–1168.

Lindhe, J., & Meyle, J. (2008). Peri-implant diseases: Consensus Report of the Sixth European Workshop on Periodontology. *Journal of Clinical Periodontology*, *35*, 282–285.

Linkevicius, T., & Apse, P. (2008). Influence of abutment material on stability of peri-implant tissues: a systematic review. *The International Journal of Oral & Maxillofacial Implants*, *23*(3), 449–456.

Listgarten, M. A., Lang, N. P., Schroeder, H. E., & Schroeder, A. (1991). Periodontal tissues and their counterparts around endosseous implants. *Clinical Oral Implants Research*, *2*(3), 1–19.

Liu, X., Zhao, X., Li, B., Cao, C., Dong, Y., Ding, C., & Chu, P. K. (2008). UV-irradiation-induced bioactivity on TiO2coatings with nanostructural surface. *Acta Biomaterialia*, *4*(3), 544–552.

Löe, H., Theilade, E., & Jensen, S. B. (1965). Experimental Gingivitis in Man. *Journal of Periodontology*, *36*(3), 177–187.

Mäkelä, M., Salo, T., & Larjava, H. (1998). MMP-9 from

TNFα-Stimulated Keratinocytes Binds to Cell Membranes and Type I Collagen: A Cause for Extended Matrix Degradation in Inflammation? *Biochemical and Biophysical Research Communications*, *253*(2), 325–335.

Maté Sánchez de Val, J. E., Gómez-Moreno, G., Pérez-Albacete Martínez, C., Ramírez-Fernández, M. P., Granero-Marín, J. M., Gehrke, S. A., & Calvo-Guirado, J. L. (2016). Peri-implant tissue behavior around non-titanium material: Experimental study in dogs. *Annals of Anatomy - Anatomischer Anzeiger*, *206*, 104–109.

Mekayarajjananonth, T., & Winkler, S. (1999). Contact Angle Measurement on Dental Implant Biomaterials. *Journal of Oral Implantology*, *25*(4), 230–236.

Meretoja, V. V., Rossi, S., Peltola, T., Pelliniemi, L. J., & Närhi, T. O. (2010). Adhesion and proliferation of human fibroblasts on sol-gel coated titania. *Journal of Biomedical Materials Research Part A*, *95A*(1), 269–275.

Meyer, S., Giannopoulou, C., Courvoisier, D., Schimmel, M., Müller, F., & Mombelli, A. (2017). Experimental mucositis and experimental gingivitis in persons aged 70 or over. Clinical and biological responses. *Clinical Oral Implants Research*, *28*(8), 1005–1012.

Milleret, V., Buzzi, S., Gehrig, P., Ziogas, A., Grossmann, J., Schilcher, K., … Ehrbar, M. (2015). Protein adsorption steers blood contact activation on engineered cobalt chromium alloy oxide layers. *Acta Biomaterialia*, *24*, 343–351.

Moon, I. S., Berglundh, T., Abrahamsson, I., Linder, E., & Lindhe, J. (1999). The barrier between the keratinized mucosa and the dental implant. An experimental study in the dog. *Journal of Clinical Periodontology*, *26*(10), 658–663.

Nakamura, K., Kanno, T., Milleding, P., & Ortengren, U. (2010). Zirconia as a dental implant abutment material: a systematic review. *The International Journal of Prosthodontics*, *23*(4), 299–309.

Nascimento, C. do, Pita, M. S., Fernandes, F. H. N. C., Pedrazzi, V., de Albuquerque Junior, R. F., & Ribeiro, R. F. (2014). Bacterial adhesion on the titanium and zirconia abutment surfaces. *Clinical Oral Implants Research*, *25*(3), 337–343.

Nothdurft, F. P., Fontana, D., Ruppenthal, S., May, A., Aktas, C., Mehraein, Y., … Kaestner, L. (2015). Differential Behavior of Fibroblasts and Epithelial Cells on Structured Implant Abutment Materials: A Comparison of Materials and Surface Topographies. *Clinical Implant Dentistry and Related Research*, *17*(6), 1237–1249.

Ong, J. L., Carnes, D. L., & Bessho, K. (2004). Evaluation of titanium plasma-sprayed and plasma-sprayed hydroxyapatite implants in vivo. *Biomaterials*, *25*(19), 4601–4606.

Oshida, Y., Hashem, A., Nishihara, T., & Yapchulay, M. V. (1994). Fractal dimension analysis of mandibular bones: toward a morphological compatibility of implants. *Bio-Medical Materials and Engineering*, *4*(5), 397–407.

Paldan, H., Areva, S., Tirri, T., Peltola, T., Lindholm, T. C., Lassila, L., … Närhi, T. O. (2008a). Soft tissue attachment on sol-gel-treated titanium implants in vivo. *Journal of Materials Science: Materials in Medicine*, *19*(3), 1283–1290.

Paldan, H., Areva, S., Tirri, T., Peltola, T., Lindholm, T. C., Lassila, L., … Närhi, T. O. (2008b). Soft tissue attachment on sol–gel-treated titanium implants in vivo. *Journal of Materials Science: Materials in Medicine*, *19*(3), 1283–1290.

Park, J. Y., & Davies, J. E. (2000). Red blood cell and platelet interactions with titanium implant surfaces. *Clinical Oral Implants Research*, *11*(6), 530–539.

Park, Y.-S., Yi, K.-Y., Lee, I.-S., Han, C.-H., & Jung, Y.-C. (2005). The effects of ion beam-assisted deposition of hydroxyapatite on the grit-blasted surface of endosseous implants in rabbit tibiae. *The International Journal of Oral & Maxillofacial Implants*, *20*(1), 31–38.

Patel, S. B., Baker, N., Marques, I., Hamlekhan, A., Mathew, M. T., Takoudis, C., … Shokuhfar, T. (2017). Transparent TiO 2 nanotubes on zirconia for biomedical applications. *RSC Advances*, *48*(7), 30397–30410.

Pätsi, M. E., Hautaniemi, J. A., Rahiala, H. M., Peltola, T. O., & Kangasniemi, I. M. O. (1998). Bonding Strengths of Titania Sol-Gel Derived Coatings on Titanium. *Journal of Sol-Gel Science and Technology*, *11*(1), 55–66.

Peltola, T., Jokinen, M., Rahiala, H., Pätsi, M., Heikkilä, J., Kangasniemi, I., & Yli-Urpo, A. (2000). Effect of aging time of sol on structure and in vitro calcium phosphate formation of sol-gel-derived titania films. *Journal of Biomedical Materials Research*, *51*(2), 200–208.

Peterson, B. W., He, Y., Ren, Y., Zerdoum, A., Libera, M. R., Sharma, P. K., … Busscher, H. J. (2015). Viscoelasticity of biofilms and their recalcitrance to mechanical and chemical challenges. *FEMS Microbiology Reviews*, *39*(2), 234–245.

Piconi, C., Burger, W., Richter, H. G., Cittadini, A., Maccauro, G., Covacci, V., … Marmo, E. (1998). Y-TZP ceramics for artificial joint replacements. *Biomaterials*, *19*(16), 1489–1494.

Piconi, C., & Maccauro, G. (1999). Zirconia as a ceramic biomaterial. *Biomaterials*, *20*(1), 1–25.

Pittayachawan, P., McDonald, A., Young, A., & Knowles, J. C. (2009). Flexural strength, fatigue life, and stress-induced phase transformation study of Y-TZP dental ceramic. *Journal of Biomedical Materials Research Part B: Applied Biomaterials*, *88B*(2), 366–377.

Ponsonnet, L., Reybier, K., Jaffrezic, N., Comte, V., Lagneau, C., Lissac, M., & Martelet, C. (2003). Relationship between surface properties (roughness, wettability) of titanium and titanium alloys and cell behaviour. *Materials Science and Engineering: C*, *23*(4), 551–560.

Pontoriero, R., Tonelli, M. P., Carnevale, G., Mombelli, A., Nyman, S. R., & Lang, N. P. (1994). Experimentally induced peri-implant mucositis. A clinical study in humans. *Clinical Oral Implants Research*, *5*(4), 254–259.

Porter, D. L., & Heuer, A. H. (1977). Mechanisms of Toughening Partially Stabilized Zirconia (PSZ). *Journal of the American Ceramic Society*, *60*(3–4), 183–184.

Prestipino, V., & Ingber, A. (1993a). Esthetic high-strength implant abutments. Part I. *Journal of Esthetic Dentistry*, *5*(1), 29–36.

Prestipino, V., & Ingber, A. (1993b). Esthetic high-strength implant abutments. Part II. *Journal of Esthetic Dentistry*, *5*(2), 63–68.

Quirynen, M., Van Der Mei, H. C., Bollen, C. M. L., Schotte, A., Marechal, M., Doornbusch, G. I., … Van Steenberghe, D. (1993). An in vivo Study of the Influence of the Surface Roughness of Implants on the Microbiology of Supra- and Subgingival Plaque. *Journal of Dental Research*, *72*(9), 1304–1309.

Quirynen, M., Van Der Mei, H. C., Bollen, C. M. L., Van Den Bossche, L. H., Doornbusch, G. I., van Steenberghe, D., & Busscher, H. J. (1994). The Influence of Surface-Free Energy on Supra- and Subgingival Plaque Microbiology. An In Vivo Study on Implants. *Journal of Periodontology*, *65*(2), 162–167.

Redey, S. A., Nardin, M., Bernache-Assolant, D., Rey, C., Delannoy, P., Sedel, L., & Marie, P. J. (2000). Behavior of human osteoblastic cells on stoichiometric hydroxyapatite and type A carbonate apatite: Role of surface energy. *Journal of Biomedical Materials Research*, *50*(3), 353–364.

Redey, S. A., Razzouk, S., Rey, C., Bernache-Assollant, D., Leroy, G., Nardin, M., & Cournot, G. (1999). Osteoclast adhesion and activity on synthetic hydroxyapatite, carbonated hydroxyapatite, and natural calcium carbonate: Relationship to surface energies. *Journal of Biomedical Materials Research*, *45*(2), 140–147.

Reheman, A., Gross, P., Yang, H., Chen, P., Allen, D., Leytin, V., … Ni, H. (2005). Vitronectin stabilizes thrombi and vessel occlusion but plays a dual role in platelet aggregation. *Journal of Thrombosis and Haemostasis*, *3*(5), 875–883.

Renvert, S., & Quirynen, M. (2015). Risk indicators for peri-implantitis. A narrative review. *Clinical Oral Implants Research*, *26*, 15–44.

Rimondini, L., Cerroni, L., Carrassi, A., & Torricelli, P. (2002). Bacterial colonization of zirconia ceramic surfaces: an in vitro and in vivo study. *The International Journal of Oral & Maxillofacial Implants*, *17*(6), 793–798.

Ritter, J. E. (1995). Predicting lifetimes of materials and material structures. *Dental Materials*, *11*(2), 142–146.

Ritzberger, C., Apel, E., Höland, W., Peschke, A., Rheinberger, V., Ritzberger, C., … Rheinberger, V. M. (2010). Properties and Clinical Application of Three Types of Dental Glass-Ceramics and Ceramics for CAD-CAM Technologies. *Materials*, *3*(6), 3700–3713.

Roccuzzo, M., Bonino, F., Aglietta, M., & Dalmasso, P. (2012). Ten-year results of a three arms prospective cohort study on implants in periodontally compromised patients. Part 2: clinical results. *Clinical Oral Implants Research*, *23*(4), 389–395.

Rompen, E., Domken, O., Degidi, M., Farias Pontes, A. E., & Piattelli, A. (2006). The effect of material characteristics, of surface topography and of implant components and connections on soft tissue integration: a literature review. *Clinical Oral Implants Research*, *17*(S2), 55–67.

Roos-Jansaker, A.-M., Lindahl, C., Renvert, H., & Renvert, S. (2006). Nine- to fourteen-year follow-up of implant treatment. Part II: presence of peri-implant lesions. *Journal of Clinical Periodontology*, *33*(4), 290–295.

Roos-Jansaker, A.-M., Renvert, H., Lindahl, C., & Renvert, S. (2006). Nine- to fourteen-year follow-up of implant treatment. Part III: factors associated with peri-implant lesions. *Journal of Clinical*

Periodontology, *33*(4), 296–301.

Roos-Jansaker, A. M., Lindahl, C., Renvert, H., & Renvert, S. (2006). Nine- to fourteen-year follow-up of implant treatment. Part I: implant loss and associations to various factors. *Journal of Clinical Periodontology*, *33*(4), 283–289.

Rossi, S., Tirri, T., Paldan, H., Kuntsi-Vaattovaara, H., Tulamo, R., & Närhi, T. (2008). Peri-implant tissue response to TiO2 surface modified implants. *Clinical Oral Implants Research*, *19*(4), 348–355.

Roy, R. K., Choi, H. W., Yi, J. W., Moon, M.-W., Lee, K.-R., Han, D. K., … Hasebe, T. (2009). Hemocompatibility of surface-modified, silicon-incorporated, diamond-like carbon films. *Acta Biomaterialia*, *5*(1), 249–256.

Ruardy, T. G., Schakenraad, J. M., van der Mei, H. C., & Busscher, H. J. (1995). Adhesion and spreading of human skin fibroblasts on physicochemically characterized gradient surfaces. *Journal of Biomedical Materials Research*, *29*(11), 1415–1423.

Rupp, F., Gittens, R. A., Scheideler, L., Marmur, A., Boyan, B. D., Schwartz, Z., & Geis-Gerstorfer, J. (2014). A review on the wettability of dental implant surfaces I: Theoretical and experimental aspects. *Acta Biomaterialia*, *10*(7), 2894–2906.

Rupp, F., Liang, L., Geis-Gerstorfer, J., Scheideler, L., & Hüttig, F. (2018). Surface characteristics of dental implants: A review. *Dental Materials*, *34*(1), 40–57.

Saber-Sheikh, K., Clarke, R. L., & Braden, M. (1999). Viscoelastic properties of some soft lining materials. I--Effect of temperature. *Biomaterials*, *20*(9), 817–822.

Salihoglu, U., Boynuegri, D., Engin, D., Duman, A. N., Gokalp, P., & Balos, K. (2011). Bacterial adhesion and colonization differences between zirconium oxide and titanium alloys: an in vivo human study. *The International Journal of Oral & Maxillofacial Implants*, *26*(1), 101–107.

Salvi, G. E., Aglietta, M., Eick, S., Sculean, A., Lang, N. P., & Ramseier, C. A. (2012). Reversibility of experimental peri-implant mucositis compared with experimental gingivitis in humans. *Clinical Oral Implants Research*, *23*(2), 182–190.

Salvi, G. E., Bosshardt, D. D., Lang, N. P., Abrahamsson, I., Berglundh, T., Lindhe, J., … Donos, N. (2015). Temporal sequence of hard and soft tissue healing around titanium dental implants. *Periodontology 2000*, *68*(1), 135–152.

Sawase, T., Jimbo, R., Baba, K., Shibata, Y., Ikeda, T., & Atsuta, M. (2008). Photo-induced hydrophilicity enhances initial cell behavior and early bone apposition. *Clinical Oral Implants Research*, *19*(5), 491–496.

Scarano, A., Piattelli, M., Caputi, S., Favero, G. A., & Piattelli, A. (2004). Bacterial Adhesion on Commercially Pure Titanium and Zirconium Oxide Disks: An In Vivo Human Study. *Journal of Periodontology*, *75*(2), 292–296.

Schakenraad, J. M., Busscher, H. J., Wildevuur, C. R., & Arends, J. (1988). Thermodynamic aspects of cell spreading on solid substrata. *Cell Biophysics*, *13*(1), 75–91.

Schakenraad, J. M., Busscher, H. J., Wildevuur, C. R. H., & Arends, J. (1986). The influence of substratum surface free energy on growth and spreading of human fibroblasts in the presence and absence of serum proteins. *Journal of Biomedical Materials Research*, *20*(6), 773–784.

Scheideler, L., Rupp, F., Wendel, H. P., Sathe, S., & Geis-Gerstorfer, J. (2007). Photocoupling of fibronectin to titanium surfaces influences keratinocyte adhesion, pellicle formation and thrombogenicity. *Dental Materials*, *23*(4), 469–478.

Schroeder, H. E., & Listgarten, M. A. (1977). *2nd, revised edition, Fine structure of the developing epithelial attachment of human teeth.* In Sauer H.W. Monographs in Developmental Biology, Vol. 2, Basel, Switzerland, S. Karger.

Schroeder, H. E., & Listgarten, M. A. (1997). The gingival tissues: the architecture of periodontal protection. *Periodontology 2000*, *13*(1), 91–120.

Schupbach, P., & Glauser, R. (2007). The defense architecture of the human periimplant mucosa: A histological study. *The Journal of Prosthetic Dentistry*, *97*(6), S15–S25.

Schwarz, F., Derks, J., Monje, A., & Wang, H.-L. (2018). Peri-implantitis. *Journal of Clinical Periodontology*, *45*, S246–S266.

Schwitalla, A. D., Abou-Emara, M., Spintig, T., Lackmann, J., & Müller, W. D. (2015). Finite element analysis of the biomechanical effects of PEEK dental implants on the peri-implant bone. *Journal of Biomechanics*, *48*(1), 1–7.

Schwitalla, A., & Müller, W.-D. (2013). PEEK Dental Implants: A Review of the Literature. *Journal of Oral Implantology*, *39*(6), 743–749.

Sculean, A., Gruber, R., & Bosshardt, D. D. (2014). Soft

tissue wound healing around teeth and dental implants. *Journal of Clinical Periodontology*, *41*, S6–S22.

Shahmiri, R., Standard, O. C., Hart, J. N., & Sorrell, C. C. (2018). Optical properties of zirconia ceramics for esthetic dental restorations: A systematic review. *The Journal of Prosthetic Dentistry*, *119*(1), 36–46.

Sivaraman, K., Chopra, A., Narayan, A. I., & Balakrishnan, D. (2017). Is zirconia a viable alternative to titanium for oral implant? A critical review. *Journal of Prosthodontic Research*, *62*(2), 121–133.

Sul, Y.-T., Johansson, C., & Albrektsson, T. (2006). Which surface properties enhance bone response to implants? Comparison of oxidized magnesium, TiUnite, and Osseotite implant surfaces. *The International Journal of Prosthodontics*, *19*(4), 319–328.

Sul, Y.-T., Johansson, C. B., Jeong, Y., Wennerberg, A., & Albrektsson, T. (2002). Resonance frequency and removal torque analysis of implants with turned and anodized surface oxides. *Clinical Oral Implants Research*, *13*(3), 252–259.

Sul, Y.-T., Johansson, C. B., Röser, K., & Albrektsson, T. (2002). Qualitative and quantitative observations of bone tissue reactions to anodised implants. *Biomaterials*, *23*(8), 1809–1817.

Sul, Y.-T., Johansson, C., Byon, E., & Albrektsson, T. (2005). The bone response of oxidized bioactive and non-bioactive titanium implants. *Biomaterials*, *26*(33), 6720–6730.

Surmenev, R. A., Surmeneva, M. A., Grubova, I. Y., Chernozem, R. V., Krause, B., Baumbach, T., … Epple, M. (2017). RF magnetron sputtering of a hydroxyapatite target: A comparison study on polytetrafluorethylene and titanium substrates. *Applied Surface Science*, *414*, 335–344.

Takami, Y., Yamane, S., Makinouchi, K., Otsuka, G., Glueck, J., Benkowski, R., & Nosé, Y. (1998). Protein adsorption onto ceramic surfaces. *Journal of Biomedical Materials Research*, *40*(1), 24–30.

Tanner, J., Carlén, A., Söderling, E., & Vallittu, P. K. (2003). Adsorption of parotid saliva proteins and adhesion of *Streptococcus mutans* ATCC 21752 to dental fiber-reinforced composites. *Journal of Biomedical Materials Research Part B: Applied Biomaterials*, *66B*(1), 391–398.

Teughels, W., Van Assche, N., Sliepen, I., & Quirynen, M. (2006). Effect of material characteristics and/or surface topography on biofilm development. *Clinical Oral Implants Research*, *17*(S2), 68–81.

Thevenot, P., Hu, W., & Tang, L. (2008). Surface chemistry influences implant biocompatibility. *Current Topics in Medicinal Chemistry*, *8*(4), 270–280.

Thomas, K. A., Kay, J. F., Cook, S. D., & Jarcho, M. (1987). The effect of surface macrotexture and hydroxylapatite coating on the mechanical strengths and histologic profiles of titanium implant materials. *Journal of Biomedical Materials Research*, *21*(12), 1395–1414.

Tiwari, A., & Hassan, M. M. (2018). Antimicrobial Coatings for Textiles. *Handbook of Antimicrobial Coatings*, 321–355.

Tomasi, C., Tessarolo, F., Caola, I., Piccoli, F., Wennström, J. L., Nollo, G., & Berglundh, T. (2016). Early healing of peri-implant mucosa in man. *Journal of Clinical Periodontology*, *43*(10), 816–824.

Tsai, I. Y., Tomczyk, N., Eckmann, J. I., Composto, R. J., & Eckmann, D. M. (2011). Human plasma protein adsorption onto dextranized surfaces: A two-dimensional electrophoresis and mass spectrometry study. *Colloids and Surfaces B: Biointerfaces*, *84*(1), 241–252.

van Brakel, R., Cune, M. S., van Winkelhoff, A. J., de Putter, C., Verhoeven, J. W., & van der Reijden, W. (2011). Early bacterial colonization and soft tissue health around zirconia and titanium abutments: an in vivo study in man. *Clinical Oral Implants Research*, *22*(6), 571–577.

van Brakel, R., Meijer, G. J., Verhoeven, J. W., Jansen, J., de Putter, C., & Cune, M. S. (2012). Soft tissue response to zirconia and titanium implant abutments: an in vivo within-subject comparison. *Journal of Clinical Periodontology*, *39*(10), 995–1001.

Vigolo, P., Givani, A., Majzoub, Z., & Cordioli, G. (2006). A 4-Year Prospective Study to Assess Peri-Implant Hard and Soft Tissues Adjacent to Titanium Versus Gold-Alloy Abutments in Cemented Single Implant Crowns. *Journal of Prosthodontics*, *15*(4), 250–256.

Watanabe, H., Saito, K., Kokubun, K., Sasaki, H., & Yoshinari, M. (2012). Change in surface properties of zirconia and initial attachment of osteoblastlike cells with hydrophilic treatment. *Dental Materials Journal*, *31*(5), 806–814.

Webb, K., Hlady, V., & Tresco, P. A. (1998). Relative importance of surface wettability and charged functional groups on NIH 3T3 fibroblast

attachment, spreading, and cytoskeletal organization. *Journal of Biomedical Materials Research*, *41*(3), 422–430.

Weber, H.-P., & Cochran, D. L. (1998). The soft tissue response to osseointegrated dental implants. *The Journal of Prosthetic Dentistry*, *79*(1), 79–89.

Wen, C. E., Xu, W., Hu, W. Y., & Hodgson, P. D. (2007). Hydroxyapatite/titania sol–gel coatings on titanium–zirconium alloy for biomedical applications. *Acta Biomaterialia*, *3*(3), 403–410.

Wennerberg, A., & Albrektsson, T. (2009). Effects of titanium surface topography on bone integration: a systematic review. *Clinical Oral Implants Research*, *20*, 172–184.

Wennerberg, A., Fröjd, V., Olsson, M., Nannmark, U., Emanuelsson, L., Johansson, P., … Thomsen, P. (2011). Nanoporous TiO2 Thin Film on Titanium Oral Implants for Enhanced Human Soft Tissue Adhesion: A Light and Electron Microscopy Study. *Clinical Implant Dentistry and Related Research*, *13*(3), 184–196.

Willbold, E., & Witte, F. (2010). Histology and research at the hard tissue–implant interface using Technovit 9100 New embedding technique. *Acta Biomaterialia*, *6*(11), 4447–4455.

Wong, J. W., Gallant-Behm, C., Wiebe, C., Mak, K., Hart, D. A., Larjava, H., & Häkkinen, L. (2009). Wound healing in oral mucosa results in reduced scar formation as compared with skin: Evidence from the red duroc pig model and humans. *Wound Repair and Regeneration*, *17*(5), 717–729.

Yang, Y., Kim, K.-H., & Ong, J. L. (2005). A review on calcium phosphate coatings produced using a sputtering process—an alternative to plasma spraying. *Biomaterials*, *26*(3), 327–337.

Yildirim, M., Edelhoff, D., Hanisch, O., & Spiekermann, H. (2000). Ceramic abutments--a new era in achieving optimal esthetics in implant dentistry. *The International Journal of Periodontics & Restorative Dentistry*, *20*(1), 81–91.

Young, T. (1805). An Essay on the Cohesion of Fluids. *Philosophical Transactions of the Royal Society of London*, *95*(0), 65–87.

Zheng, M., Yang, Y., Liu, X.-Q., Liu, M.-Y., Zhang, X.-F., Wang, X., … Tan, J.-G. (2015). Enhanced Biological Behavior of In Vitro Human Gingival Fibroblasts on Cold Plasma-Treated Zirconia. *PloS One*, *10*(10), e0140278.

Zitzmann, N. U., & Berglundh, T. (2008). Definition and prevalence of peri-implant diseases. *Journal of Clinical Periodontology*, *35*, 286–291.

Zitzmann, N. U., Berglundh, T., Marinello, C. P., & Lindhe, J. (2001). Experimental peri-implant mucositis in man. *Journal of Clinical Periodontology*, *28*(6), 517–523.

ORIGINAL PUBLICATIONS

Annales Universitatis Turkuensis

UNIVERSITY OF TURKU

Grano Oy - Turku, Finland 2019

ISBN 978-951-29-7596-9 (PRINT)
ISBN 978-951-29-7597-6 (PDF)
ISSN 0355-9483 (Print)
ISSN 2343-3213 (Online)